Graduated Bowman probe

BMEDesign: Final Report

April 29th, 2026

Biomedical Engineering 301

Section 304

Client: Dr. James Law & Dr. Suzanne Van Landingham

Advisor: Prof. Monica Ohnsorg

Team Members:

Neel Srinivasan (Leader, BPAG) | nsrinivasan8@wisc.edu

Cole Miller (Communicator) | ctmiller8@wisc.edu

Caden Robinson (BSAC) | carobinson5@wisc.edu

Caleb White (BWIG) | cfwhite@wisc.edu

Abstract

Nasolacrimal duct obstructions (NLDO) and canalicular lacerations are injuries to the lacrimal drainage system causing complications to the physiological function of the system which can lead to an assortment of adverse symptoms including epiphora and infection. Depth assessments of lacerations and NLDOs are currently performed by inserting a Bowman probe, securing the distal visible end with forceps, and measuring the exposed length with a ruler. This method introduces measurement inaccuracies due to the additional step of using a ruler to determine depth. Dr. James Law and Dr Suzanne Van Landingham of the UW-Hospital requested a version of the current probe but with graduated markings. Using a LasX 200 watt laser to create an additive oxidation layer, markings every 2.5 mm were implemented onto the surface of the probe. This device was tested against 4 main specifications of which were, uniform and consistent interval marking length, degradative natural biological and autoclave environments, tissue damage when used during probing, and accuracy for finding the depth of an NLDO or laceration. The test results indicated that the graduated version of the probe provided similar and in some cases, better results than the current clinical standard of measurement estimation utilizing bowman probes. Questionnaire data showed that graduated version is more favorable for usage during surgery indicating its potential in the industry. Successful implementation of this device could help provide more accurate diagnosis of NLDOs and canalicular laceration allowing for more effective treatment and lower recurrence rates.

Table of Contents

Introduction

A. Impact and Motivation

Inhibition of physiological function to the lacrimal drainage system can be caused by a variety of adverse conditions. Nasolacrimal duct obstruction (NLDO) is a common ophthalmologic condition affecting both infants and adults, often leading to chronic tearing, infection, and decreased quality of life if not properly treated. Canalicular lacerations are trauma induced tears of the lacrimal canaliculi prevalent in younger demographics, resulting in an inability to process lacrimal fluid, epiphora and possible infection. Current standard Bowman probe devices lack graduated measurement markings, forcing clinicians to estimate insertion depth during probing procedures and increasing the risk of inaccurate obstruction localization, tissue trauma, and suboptimal treatment planning. Given the frequency of lacrimal procedures and the delicate anatomy of the nasolacrimal system, a graduated probe that provides precise, millimeter-scale depth feedback would reduce human error, improve diagnostic accuracy, and support more personalized and effective patient care across diverse age groups and clinical settings.

B. Existing Designs

There are currently no graduated Bowman's probes meant for clinical use available on the market. The current clinical 'gold standard' for obtaining lacrimal measurements is through use of an ungraduated traditional probe where quantitative values are ascertained through comparison to an external measuring apparatus, most commonly a ruler. This form of measurement introduces the possibility of transfer error and can easily be streamlined through combination of the two components. There are a few graduated designs which have been developed for research-based deployment. The Calibrated Bowman's Lacrimal probe from the All India Institute of Medical Sciences is a set of Bowman's probes that feature laser engraved numbers at varying millimeter intervals [1]. This design maintains ISO-10993-1 standards for biocompatibility and easily distinguishable millimeter markings for probe insertion depth into the nasolacrimal duct. This design does not exactly fit the criteria and function that has been requested by the client, as expanded upon in Background Section C: Design Specifications.

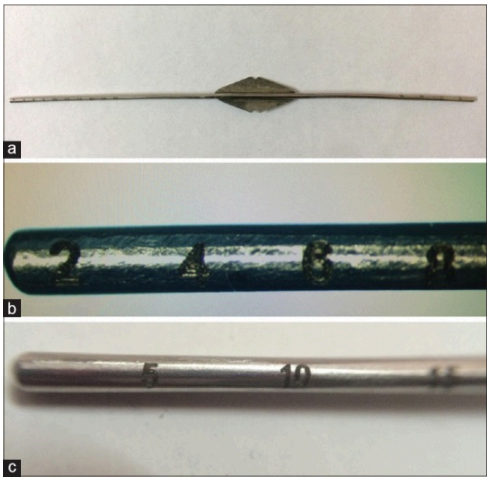

Figure 1: Calibrated Bowman's Lacrimal probe from the All India Institute of Medical Sciences [1]

C. Problem Statement

There are currently no available graduated Bowman's probes available for clinical use on the market. Consequently, doctors performing clinical procedures requiring lacrimal measurements are required to rely on external measuring methods to estimate probe insertion depth. This indirect approach introduces user-dependent variability and measurement uncertainty, particularly in cases involving partial obstruction, canalicular narrowing, or atypical anatomy, where tactile feedback alone may be difficult to interpret. These limitations are recognized contributors to occasional mislocalization of damage which can result in unnecessary invasive surgical intervention, increased medical costs, and patient discomfort. To provide an easier method of measurement acquisition, the creation of a set of clinically accessible graduated Bowman's probes is necessary. By creating an accurate device that features easy data collection, doctors will be able to ascertain the exact location of lacrimal measurements which will allow for the prescription of more personalized treatment plans to patients. The device must be identical in dimensions to currently used Bowman's probes, feature distinguishable markings, and minimize any changes to surface texture in order to maximize measurement accuracy and patient safety.

Background

A. Relevant Biology and Physiology

The lacrimal drainage system is the anatomical irrigation pathway that removes tears from the ocular surface to the nasal cavity, intrinsic to keeping the eyes lubricated, nourished, and protected [2]. The system includes the lacrimal gland and excretory ducts which are located oblique to the eye as well as the puncta, canaliculi, lacrimal sac, and nasolacrimal duct, all of which reside between the eye and the nose [2]. When proper physiological function of this system is inhibited, propagation of infection and immunogenic response follows, damaging the health and wellbeing of the patient. Inhibition of lacrimal function can come through a variety of sources including any level of trauma or blockage. Blockages within this system are known as nasolacrimal duct obstructions, or more simply lacrimal obstructions, and can lead to an assortment of symptoms, such as epiphora (excessive tearing) and infection, which may result in the need for invasive surgical intervention [3]. During gestation, a cord of ectodermal tissue separates from the surface and enters grooves between the frontons and maxillary processes of the eye. This tissue eventually canalizes and forms the lacrimal sac and nasolacrimal duct of the lacrimal drainage system, fully developing by birth [4]. Incomplete canalization is the most common cause of nasolacrimal duct obstruction, where the puncta is clogged [5]. With age, inflammation, and injury, this tube can get even narrower which leads to the duct being obstructed, resulting in the aforementioned symptomology. Nasolacrimal duct obstructions are an incredibly common disorder of the lacrimal system; between 6 to 20 percent of newborns exhibit symptoms [6]. The condition can be treated with several methods including ointments, gentle massaging, and eye drops [7]. Commonly, however, symptomology continues to persist despite application of these known remedies, creating the necessity for a consistent solution in ophthalmological procedure. To treat the issue, doctors will use a Bowman probe to gauge where the obstruction is and assess what type of treatment and operations are required. For effective probing, an ophthalmologist must pass the probe through the bony nasolacrimal canal and perforate the embryological membrane without traumatizing other anatomical structures or creating a false passage [8]. Accurate evaluation

of nasolacrimal blockages through the use of Bowman probes is necessary for appropriate treatment evaluation and quick patient recovery to minimize patient discomfort.

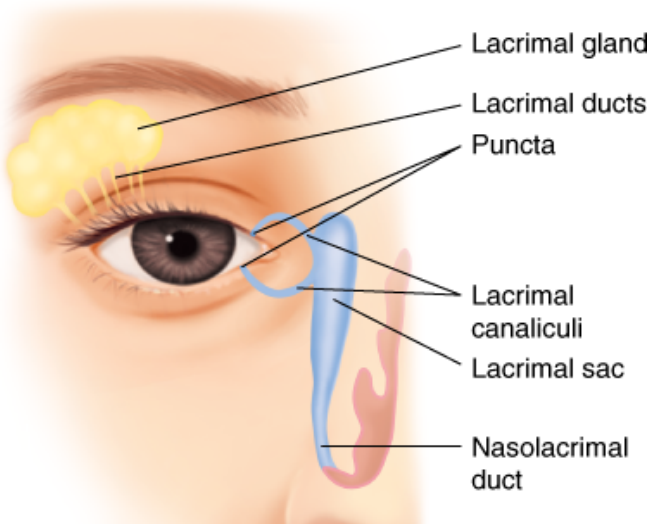

Figure 2: Diagram of the Nasolacrimal drainage system [9]

Less common, but just as impactful for consideration, are canalicular lacerations. These lacerations are most commonly created from traumatic tears of the lacrimal system induced by eyelid trauma, accidents, or dog bites [10]. Partnering approximately 20% of eye lid trauma cases, canalicular lacerations make up a significant portion of eye related hospitalizations especially in younger, male demographics [11]. The upper and lower canaliculi of an individual are located within the medial aspects of both eyelids, adjacent to the eyes' puncta, and millimeters from surface epithelium, leaving them susceptible to harm during traumatic accidents [12]. Laceration of the canaliculi reduces the lacrimal system's ability to transport tears from the eye to the nose and can result in significant pain, epiphora, and infection of the individual. Bowman probes are used to assess these lacerations through fine insertion in through the associating eye’s punctum. Once inside, the clinician will continue to insert the probe distally until the point of laceration is identified [13]. This insertion depth is then measured using an external measuring apparatus and the patient's treatment plan is then curated with consideration to extraneous damage. Deep rooted lacerations which slice near the soft tissue lacrimal sac are most commonly prescribed OR treatment, requiring intense anesthesia and hefty medical costs. Shallower lacerations found closer to the punctum are generally prescribed ER treatment which utilize only local anesthesia and are often much cheaper [14]. Diagnostic accuracy of the surgical intervention format is therefore a determinant of surgical invasivity, medical availability, and patient preference of both health and financial considerations. It is therefore imperative that the Bowman probe measurement procedure is as precise and accurate as possible.

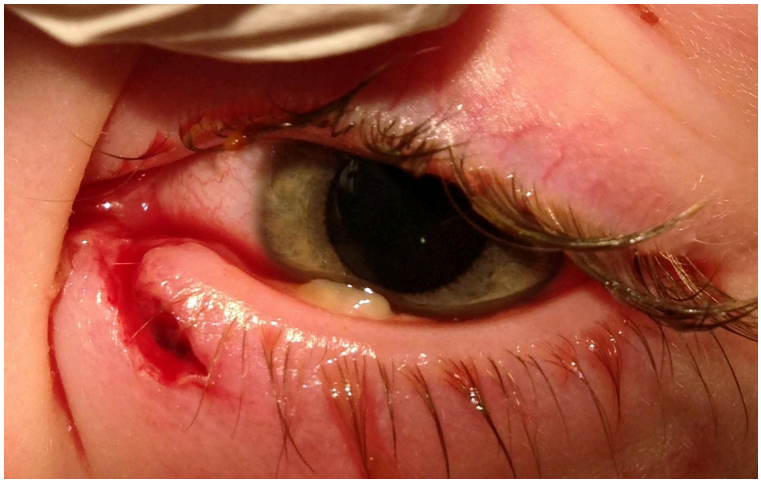

Figure 3: Canicular laceration resulting from trauma to the lower eyelid[15]

B. Client Information

The client, Dr. James Law, is an oculofacial plastic surgery fellow in the UW Madison Department of Ophthalmology and Visual Sciences. The alternate client, Dr. Suzanne van Landingham, is an associate professor & oculoplastic surgeon in the UW Madison Department of Ophthalmology and Visual Sciences. Their clinical demographic for lacrimal procedures is primarily adults. They are interested in getting access to a probe that will allow quantitative characterization of lacrimal duct obstruction depth during procedure.

C. Design Specifications

The client has requested a set of graduated Bowman's probes that allow for quick and accurate diagnostic measurements of the lacrimal system. The device must comply with ISO-13485:2016 and ISO-10993-1 which requires manufacturing uniformity and biocompatibility across all prototypes respectively [16]. The final design must feature visible markings up to 35 mm at 5 mm intervals without changes to the surface texture as requested by the client. Further, the markings themselves must be within a ± 0.5mm range of exact graduation spacing as outlined by ISO-2768. The device must also be able to withstand repeated autoclave cycles with an environment of 135 ℃ and 15-20 psi [17]. The prototyped set of 6 Bowman's probes must match the dimensions of standard Bowman's probes with lengths ranging from 130 - 150 mm, a target weight of 45 grams, and diameters ranging from 0.4 to 1.8 mm [18]. The client has provided a flexible budget of $100 to design & fabricate the device.

Preliminary Designs

A. Laser Engraving

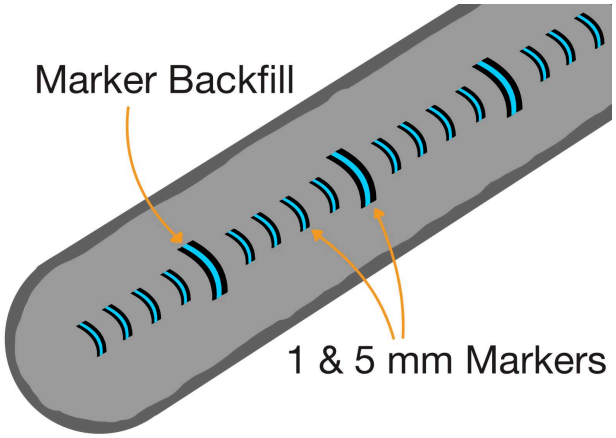

Figure 4: Laser engraving design

The first design uses laser engraving to add graduation markings to the Bowman's probe. Small hashes or dots will represent 1 and 5 mm markings along the probe, which will be made by using a laser to engrave on the probes. The markings are expected to penetrate about 50 µm into the probe so there is minimal risk in terms of structural integrity. The largest concern with this specific design is the engravings, when used during a procedure, could pull on the inner tissues of the nasolacrimal cavities causing more complications for the surgery and possible injury to the patient. To eliminate this issue, these engravings will be filled with a similar material with multiple of the same properties to smoothen the surface out. This design will be easier to fabricate compared to the designs featuring electroplating and thermochromism as laser processing requires less preparation.

B. Laser Annealing

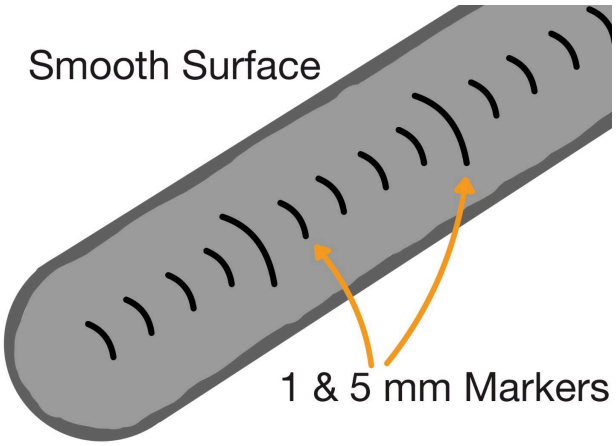

Figure 5: Laser annealing design

The second design considered uses laser annealing as a means to create line markers across the Bowman's probes surface. Laser annealing is similar to laser engraving as they both use a laser to change the appearance of a chosen surface. However, unlike laser engraving in which the surface material is removed, laser annealing maintains the original surface chemistry and texture while discoloring the surface. This difference is because laser engraving uses a higher powered laser relative to laser annealing. By focusing a low energy laser on the surface at 1 and 5 mm intervals, an oxidation layer will form causing discoloration at the accurate line markings [19]. This process will provide easily distinguishable line markers for doctors to reference during nasolacrimal duct obstruction probing procedures.

C. Electroplating

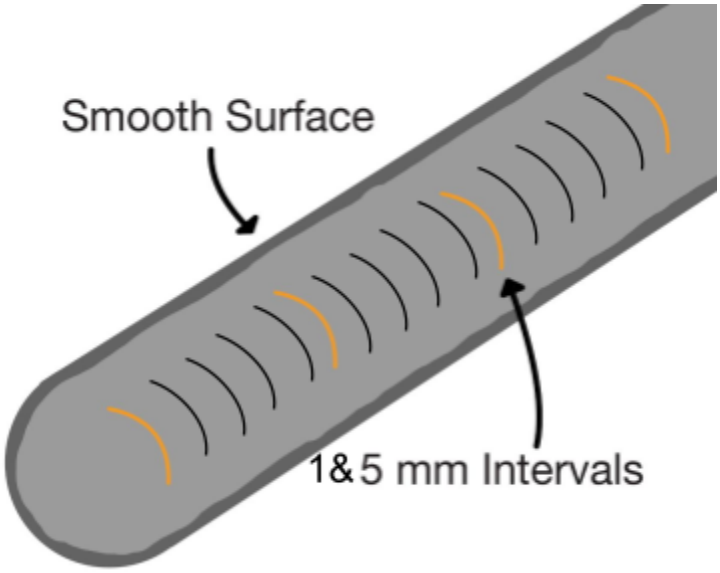

Figure 6: Electroplating design

The third design consideration is electroplating. Electroplating is the process of producing a metal coating on a solid substrate through the reduction of cations of the chosen metal via an electrical current. The two chosen substrates in this case would be the stainless steel Bowman probe, acting as the anode, and a secondary, separate colored biocompatible metal, such as a dark titanium, as the cathode [20]. Using electroplating, tiny strips of metal coating would be plated onto the Bowman probe in specific locations through controlled masking with tape or wax. These tiny strips would indicate millimeter measurement markings along the shaft of the probe, providing a visible graduation for real-time, clinical use during ophthalmological procedure.

D. Thermochromism

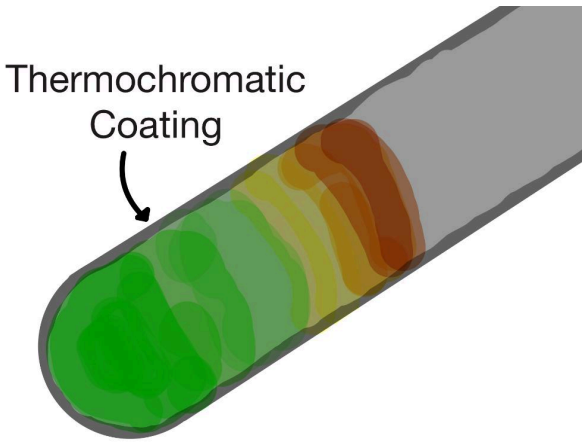

Figure 7: Thermochromism design

The final design features a thermochromatic coating that is intended to change the probe's color depending on the insertion depth into the human body. Thermochromic coatings are composed of microcapsules that contain encapsulation agents and pigments such as urea-formaldehyde and leuco dyes respectively. When heated, the solvent inside the capsules melts which allows the weak acids to interact with the leuco dyes. This process changes the capsule's chemical composition and results in the probe's surface changing color [21]. Upon use, this design would require doctors to maintain nasolacrimal duct probe insertion until the thermochromic coating activates and changes the probe's appearance. After the probes change in color, the doctor would need to measure the range of color manually with a measuring tool.

Preliminary Design Evaluation

A. Design Matrix

The most critical design specifications were considered when creating the design matrix. Criteria are weighted and ordered based on importance. The winning design was Laser Annealing.

Table 1: Design Matrix

		Laser Engraving		Laser Annealing		Electroplating		Thermochromism	
		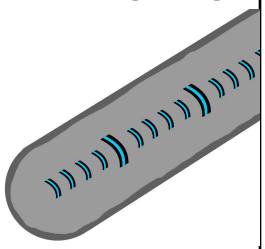		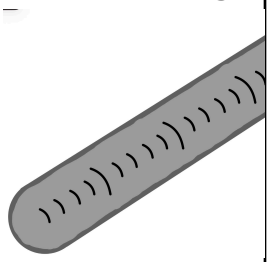		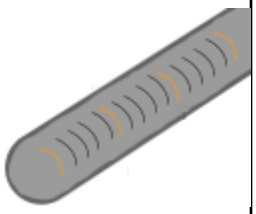		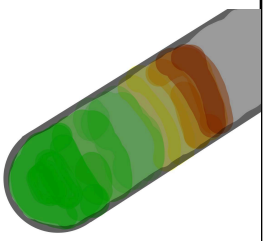	
Criteria	**Weight**	**Score**	**Weighted Score**	**Score**	**Weighted Score**	**Score**	**Weighted Score**	**Score**	**Weighted Score**
Accuracy	25	5/5	25	5/5	25	5/5	25	3/5	15
Patient Safety	25	3/5	15	4/5	20	4/5	20	2/5	10
Ease of Data Acquisition	20	5/5	20	4/5	15	3/5	12	2/5	10
Durability	15	2/5	6	5/5	15	3/5	9	3/5	9
Ease of Fabrication	10	4/5	8	2/5	4	2/5	4	3/5	6
Affordability	5	5/5	5	2/5	2	2/5	2	2/5	2
Total	**100**	SUM	**79**	SUM	**81**	SUM	**72**	SUM	**52**

B. Determination of Criteria and Justification of Scores

Accuracy - This criteria refers to the probes ability to accurately measure the depth of the probe that has been inserted into the nasolacrimal duct. Markings must be made at the correct depths, and must have the marking be easily discernible so the user reports the correct value. Accuracy is of critical importance to ensure the user is able to make accurate measurements of the depths of blockages to inform treatment. Laser Engraving, Electroplating, and Laser Annealing all scored 5/5 in accuracy, due to their precision of machining, and clearly marked depths. Thermochromism received the lowest score of 3/5 due to the less direct nature of the measurement. There are a number of factors that might influence the accuracy of the Thermochromism measurement, including diverse internal temperatures, length of exposure, and difference in how color is measured between clinicians, ultimately decreasing the accuracy of the design.

Patient Safety - Patient safety refers to the probes ability to not harm or negatively affect the patient during standard use. To ensure safety, designs must have a smooth exterior that can not get caught on anything when inserted into the nasolacrimal duct. Additionally, the probe and alterations to the probe must be biocompatible, ensuring that it has no negative effects due to chemicals or materials used. Patient Safety is tied for the highest weighting, 25%, as the probe must be safe to be a beneficial improvement to standard Bowman probes. Electroplating and Laser Annealing both scored the highest score of 4/5 due to having smooth markings that can’t catch on anything in patients. The second highest score of 3/5 was awarded to Laser Engraving, slightly lower than Electroplating, due to having engravings that could possibly catch during use. Thermochromism scored 2/5, the lowest score in this category. This is due to the use of weak acids and encapsulation agents such as urea-formaldehyde, which could have potential biocompatibility issues, especially if the surface of the probe is broken in some way.

Ease of Data Acquisition - This criterion refers to the simplicity of probe measurement. Specifically, this category assesses how easy the nasolacrimal duct insertion depth can be determined from the design. Additionally, possible fading of markings due to autoclaving or use will be considered, as this impacts the ease of use. This category is quite important as the user’s ability to easily ascertain depth insertion is of importance, hence its weighting of 20%. The laser engraving design earned the highest score of 5/5 due to its brightly colored line markings at 1 mm & 5 mm offering simple direct measuring capabilities. The laser annealing design ranked second in this category with a score of 4/5 as it offers distinguishable line markings at 1 and 5 mm. Unlike the laser engraving design, which features brightly colored backfill in the engravings, the laser annealing method scored slightly lower as it doesn’t feature this color distinction. The electroplating design placed third in the rankings at 3/5 due to its infrequent line markings. While this design features accurate line markers at 5 mm intervals, the exact measurement would prove difficult to gauge and would rely on the user's estimation. The final design featuring thermochromatic coatings scored a 2/5 in this category, the lowest of the 3 chosen designs. The rationale behind this decision is because of the lack of markings on the probe. While this design features a non-surface-penetrating method of graduation, the inverse effect is that doctors must measure the range of color change using their own measurement tools, ultimately making data acquisition more difficult.

Durability - This criterion is relatively straightforward and highlights the physical properties of the different designs of these probes. The probes must strike a delicate balance of being strong enough to prevent any form of breakage during procedure but also flexible enough to respond to patient-to-patient variability in lacrimal pathway navigation. Durability refers to the design's ability to withstand changes or degradation to either the

markings or the probe itself during sterilization and repeated use. The laser engraving design scored the lowest because both the probe's properties and structure are being manipulated. While re-coating it with a new material to smoothen out the edges seems like a good option, a new material introduced into the probe could result in increased and undesired stiffness or flexibility, which is why it scored the lowest. The other three prototypes' physical probe structure would not be manipulated with their respective graduation methods, meaning that no change will be made to the probe's structural properties, specifically with respect to stress and strain tolerance. In terms of marking durability, each of the engraving, electroplating, and thermochromatic designs contain susceptibility to longer term corrosion and degradation. Vulnerable to pitting corrosion, galvanic corrosion, and loss of coating adhesion respectively, these three designs are at risk of decreased visibility and reliability of the graduated markings over time, garnering their lower scores. The laser annealing graduation process uses laser oxidation, which can only be reverted through an additional laser procedure or intense sanding of the surface, meaning repeated sterilization and use would not alter the visibility or reliability of the graduation, at least before probe failure itself.

Ease of Fabrication - The ease of fabrication criterion refers to both the general feasibility and technical finesse required for the consistent execution of the described fabrication method. This criteria provides insight into what design ideas are realistic answers to the problem at hand, and what design ideas are built on a hypothetical solution. The design that scored highest in this criterion was the laser engraving design, earring a 4/5 . The group has experience with laser engraving and therefore understand the fundamental process associated with the specific fabrication method. Laser engraving would eliminate the human error associated with fine measurement graduation and therefore provide consistent, precise results that could be feasibly accomplished within the semester time frame despite lack of experience on the probe scale. The other designs, laser annealing, electroplating, and thermochromism, scored lower, with respective scores of 2/5, 2/5 and 3/5. All of these design ideas introduce technical practices the group is unfamiliar with which grows the opportunity for error during the fabrication process. Similarly, the electroplating and thermochromism fabrication practices require a strong chemical intuition that again may very easily introduce inaccuracy.

Affordability - The affordability criterion refers to the cost associated with the execution of each design idea. The design should desirably be cost effective in both a singular instance, and over repeated fabrications. The design that scored the highest was design 1, laser engraving. All the design requires is use of the laser at the Wendt Commons Makerspace, as well as potentially a biocompatible resin to fill in the engraving incisions to prevent tissue compromisation. The other designs each received a ⅖ score, as they would require either continuous purchase of multiple coating and fabrication materials or expensive fabrication equipment not necessarily available for free use for the group.

C. Proposed Final Design

Laser annealing is the best and most efficient approach to graduating these Bowman probes. The key aspects about this design is that it removes no material from the probe, but rather a small oxidative layer is generated creating a color change on the surface. This design scored the same in accuracy as the electroplating and laser marking options because they would gather measurements by using the same technique. It will be easily programmable to ensure that these markings are within ± 0.5mm range of graduation spacing as outlined by ISO-2768. For patient safety, this design again scored the highest due to the fact that no new material is being added or subtracted from the probe. It will maintain all qualities that ophthalmologists are used to working with in practice and adds now concerns relating to pulling on the tissues inside the nasolacrimal canals. For the next criteria, Ease of data acquisition, it scored the second highest solely because of the potential of the graduation fading during the autoclave process. Multiple testing trials will be conducted to ensure that the graduation will not fade, but still, this possibility should be considered. For durability, this design scored the highest again because no material was removed from the probes and they will maintain all physical properties they had previously. This design scored the lowest for ease of fabrication solely based on the materials present for the design team. If the specific laser annealing machine is not available, another route will have to be considered for graduation. Finally cost, annealing scored the lowest again since it is a little more expensive than laser engraving. Overall, this design, although a little more expensive than others, will provide the safest approach and easiest to replicate for graduating Bowan probes.

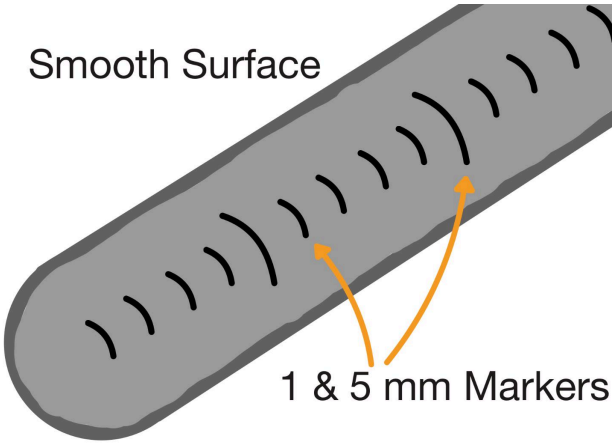

Figure 8: Proposed final prototype featuring laser annealing

Fabrication

A. Materials

Graduated Bowman's Probe

For fabrication of the graduated Bowman probe, a set of A420 medical grade stainless steel probes will be modified through a precise laser marking process using a LasX industrial 200 watt laser. Stainless steel is the standard material of application for Bowman probes, and most surgical equipment, due to its set of valuable and unique characteristics. Stainless steel has intensely high biocompatibility, durability, and malleability, something specifically important for delicate navigation through the lacrimal duct [22]. Additionally, when alloyed with a layer of chromium oxide, the steel becomes highly corrosive-resistant, significantly increasing its life span and improving its ability to be sterilized [23]. Depending on the laser frequency and the scan speed, the speed at which the laser moves across the probe, varying color changes from the oxidation process can occur, ranging from a brownish-yellow to blue[24]. Bowman probes are semi-invasive and are required to be sterilized through autoclave after each use, making this sterilization quality necessary. The laser annealing process will only be modifying the existing stainless steel on the probe and will not be adding any additional material.

Aluminum Laser Fixture

The laser fixture was fabricated from a laser-safe, nonreflective slab of 6061 aluminum. This material, while still durable, is especially easy to fabricate due to its relative softness and low density. The slab was shaved down to 9.54mm x 76.09 x 115 mm rectangular prism so it fit inside of the laser bed while still allowing the probe's center of gravity to be placed on the holder. It is the optimal material to fabricate using a CNC milling machine and requires no surface preparation before being introduced to the laser.

B. Methods

Graduated Bowman's Probe

Laser annealing is the process of slowly heating the surface of a material until chemically oxidized in order to generate a darkened color shift on the material surface. It neither takes nor adds any additional material to the item of interest, preserving the surface finish common with the rest of the item and preventing bacterial build up within the minor grooves generated in laser engraving [25]. When annealed, the layer of chromium oxide that is promoting corrosion resistance of the steel is melted off, but is quickly restored through spontaneous passivation, preserving this necessary quality [26]. Commonly used for barcodes and branding, laser annealing is a precise design method that utilizes computer generated vector files for output of a precise and clean design. A vector file, which can be developed in most common softwares, will provide the mathematical accuracy for a laser finish that is needed for the millimeter graduation desired for the probe.

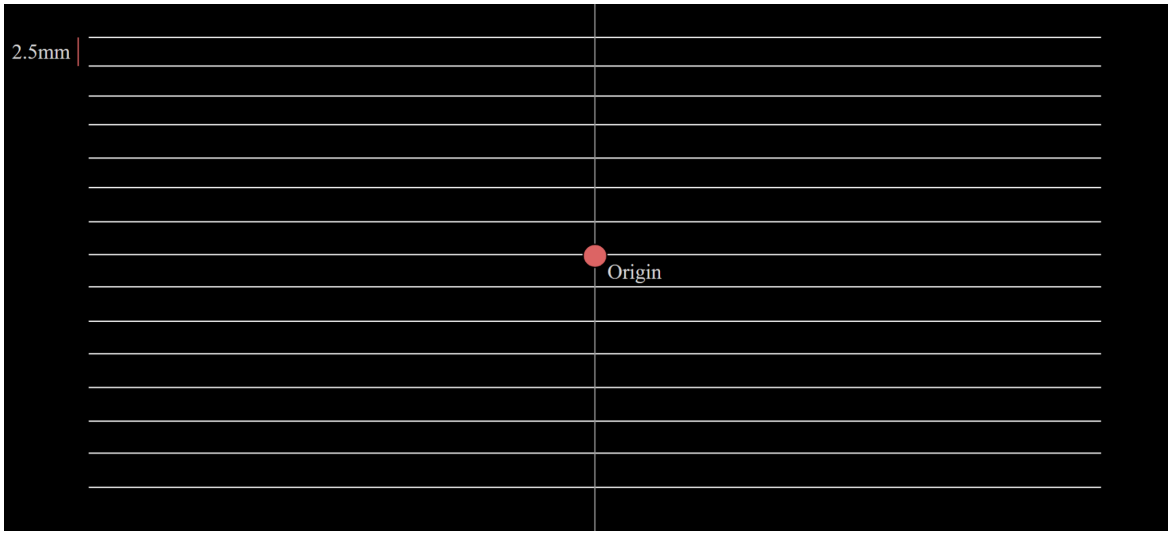

Figure 9: LasX laser vector file with 15 2.5mm spaced lines for graduated induction onto probe shafts

Aluminum Laser Fixture

An Eisen S-3AII mill with ProtoTRAX EMX was used during fabrication of the holder to create three vertical channels spaced 2 cm apart carved into the slab to ensure the probes lay flat and straight. Each vertical channel was fabricated with different depths ranging from 0.038 mm to 0.076 mm. Since each probe has a different diameter, the varying depths allow for smaller probes to be sufficiently marked, rather than sitting too deep into the slab and not receiving a full mark. Three horizontal channels, spaced 1cm apart were also added to provide consistent alignment, so the end of the probe was positioned exactly 2.5 mm from the first marking. The depth of these channels is not relevant since they are only used as a visual marker.

C. Final Prototype

The final graduated probe prototypes were a set of six, 6”, 0000-000, 00-0, 1-2, 3-4, 5-6, 7-8 sized AISI 420 German stainless steel Bowman Probes. The graduation was induced using a LasX Industries S/N 1408-001 200-watt fiber laser with 20% duty cycle, 30% power output on a 40kHz frequency with 0 background modulation and 100% depth control with the laser held at 400 mm/s translational velocity. This combination of parameters was determined through slow fabrication parameter shifting until an appropriate combination was reached. These parameters allowed the generation of visible, precise markings along the shaft of the probe with minimal influence on probe surface properties.

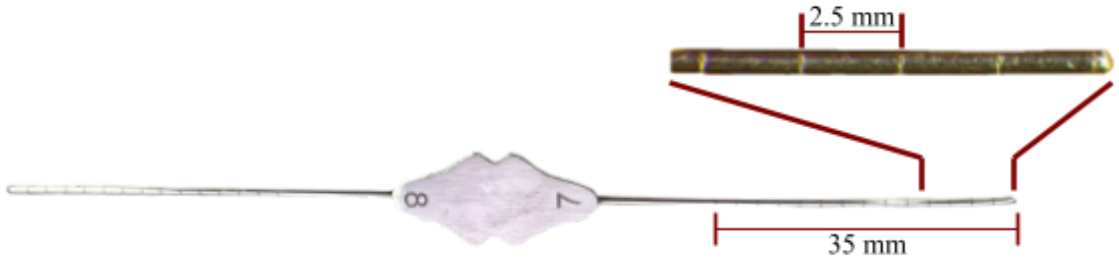

Figure 10: Final graduated Bowman’s probe prototype featuring additive 2.5mm interval markings up to 35 mm along the probe

The final laser fixture features a nonreflective slab of 6061 aluminum with three different sizes of induced probe horizontal guidance slots spaced 2 cm apart for perpendicular and consistent laser graduation induction. The slots were fabricated using a Eisen S-3AII mill with ProtoTRAX EMX measurement system to allow for ultra precise grid formation to prevent millimeter level variation in fabrication. The vertical slots are 1 cm apart and placed for consistent probe alignment to ensure that the first graduation marking is placed directly at the tip of the probe. A detailed protocol for laser fixture fabrication is outlined in Appendix H.

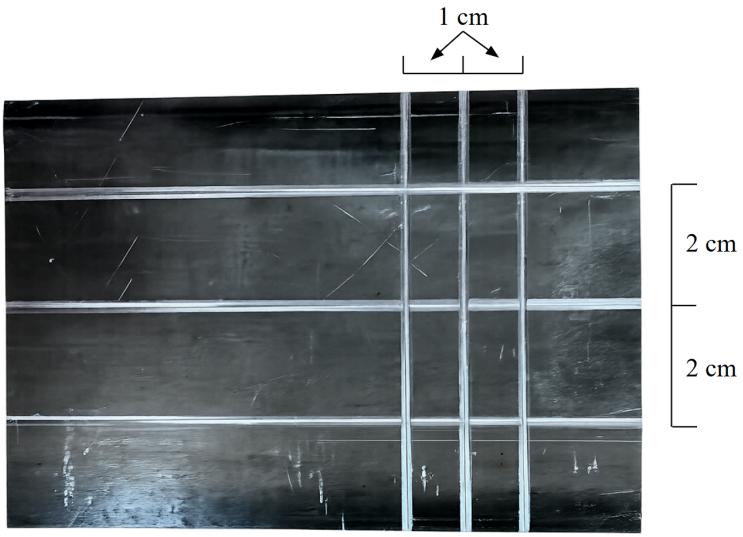

Figure 11: Final aluminum laser fixture for alignment and uniform manufacturing of graduated Bowman’s probes

Testing and Results

In order to test that the fabricated Bowman probe design satisfies all necessary PDS and client requirements, a series of both quantitative and qualitative assessments were curated. The testing procedures used to generate these conclusions include the following: a cadaveric laceration assessment; phantom soft tissue pull test, bioreactor and autoclave material deposition observations; and probe fabrication uniformity testing.

A. Cadaveric Laceration Testing

To prove the diagnostic accuracy of the graduated probes, the cadaveric laceration assessment looked to use real life probe application to demonstrate the probes equivalent capabilities to current clinical techniques. This test saw Dr. Law surgically induce a laceration somewhere along the left lower and right upper canaliculi of 5 cadaveric specimens, resulting in 10 distinct measurements. These lacerations were then measured by two medical school residents of the UWSMPH and Dr. Law using the following set of techniques: observable estimation; an ungraduated probe; an ungraduated probe in combination with an external measuring apparatus (current standard); a graduated probe.

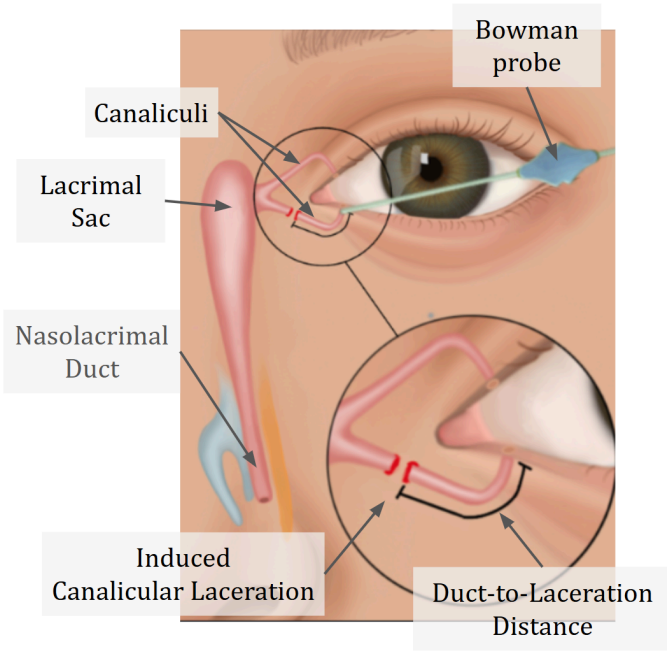

Figure 12: Diagram of canalicular laceration in the nasolacrimal drainage system

Once a technique was used, the participants reported the measurement for recording. Using the current standard as the ‘clinical’ laceration depth, each technique was evaluated in comparison to the clinical laceration depth to obtain an accuracy score defined as the absolute distance away from this value. With data for each technique, from each participant, at all 10 lacerations, two distinct statistical tests were conducted to evaluate the quantitative accuracy of the measuring techniques. The first test, was a paired TOST (two one-sided test) in order to prove equivalency between the clinical measurements and the graduated measurements. The second test was a paired t-test used to prove a difference between the ungraduated accuracy scores and the graduated accuracy scores. Combined, significant results would allow the graduated probes to be translationally defined as

an equivalent or superior method of clinical quantitative characterization of lacrimal measurements with respect to the gold standard and ungraduated measurement techniques respectively.

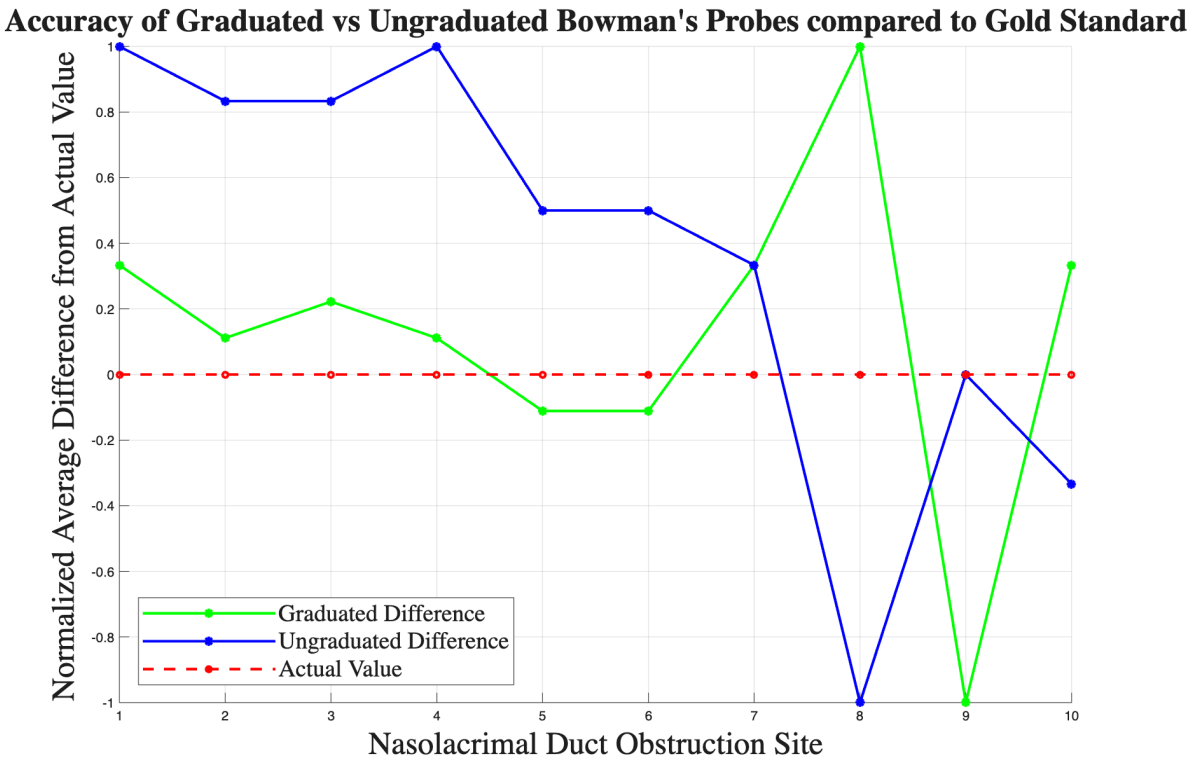

Figure 13: Accuracy scores of the graduated and ungraduated probes in reference to the clinical laceration depth for all 10 measurement locations, averaged across the three participants.

It is important to note that because the true canalicular laceration length is not directly known, absolute measurement accuracy cannot be determined. Therefore, only agreement with the current clinical standard was assessed. While paired t-tests are used to evaluate differences between methods, equivalence TOST testing with predefined clinical margins provides a more appropriate framework for determining whether the graduated probe produces measurements comparable to the standard approach. Specifically, the TOST evaluation was conducted to answer the question of whether the graduated probes produce measurements that are clinically indistinguishable from the current standard method. Because no derived constant for acceptance of clinical measurement variability exists, a delta value of 0.5 mm was applied based on the idea that a change in 0.5 mm estimation would not significantly alter the interpretation of the case. In this test, a 90% confidence interval is generated through comparing the paired difference mean across all measurements. It tracks whether or not the mean difference fails within the negligible range, between the upper and lower bounds. Using each participant's raw measurement value at each of the 10 obstruction sites for a value of n = 30, pairing each graduated value to its partnering gold standard value, the result was deemed equivalent. This means that the difference between the measurement values is small enough that the variation can be considered clinically irrelevant, therefore deeming the measurement techniques as indistinguishable in accuracy.

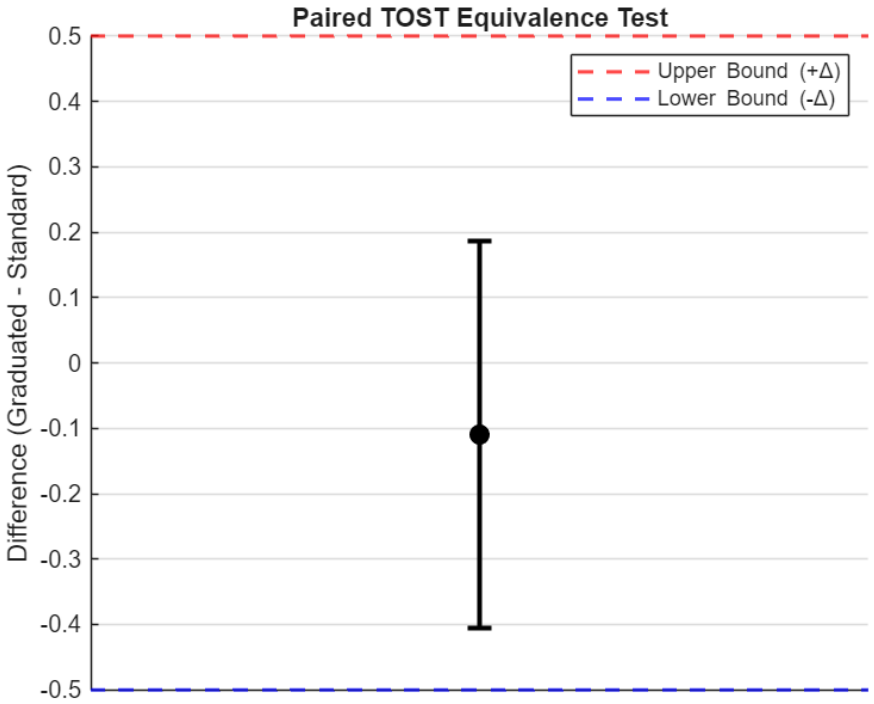

Figure 14: The 90% confidence interval for the mean paired difference fell entirely within the predefined equivalence bounds (±Δ), visually supporting the conclusion of equivalence between the graduated probes and the standard measurement method.

The second test utilized a paired t-test with a desire to reject the null hypothesis. The null hypothesis proposed that the graduated and ungraduated probe methods were equivalent in their accuracy in reference to the clinical gold standard value. Comparing each accuracy score of the graduated and ungraduated probes at each station for each participant, a p-value less than 0.05 was returned. This conclusion indicates that the supplied data sets are statistically significant, meaning the improved accuracy seen with the use of graduated probes in comparison to the ungraduated was not a result of random chance but rather a result of the graduation guiding accurate diagnostic estimation. These results confirm the usefulness of the graduated probe for both its accuracy and simplicity, imploring further push for actual implementation of the graduated probes into a clinical setting. It is important to note that testing these probes on cadavers is different from their performance on a live person, since there will be other biological factors like blood and swelling that are not accounted for. It will be crucial that these probes are tested in live patients to guarantee their effectiveness. Since the obstructions inside the cadavers were not known, determining their location required a level of operator skill. This led to variability in each measurement, as both residents and the fellow reported different depths within the same specimen. Using an actual absolute known depth could help to reduce this variability and allow for more accurate evaluation of the graduations accuracy during testing.

B. Tissue Pull Testing

The largest concern expressed by the client for laser-induced graduated was the increased risk of tissue pull. More technically defined as soft tissue damage resulting from surgical intervention during a clinical procedure, resultant tissue pull of an uneven and jagged probe exterior would leave the probe unusable because of the increased risk of patient safety. In order to test whether or not the laser-induced graduation would result in significant lacrimal soft tissue damage, development of a soft tissue disruption procedure was generated. This procedure involves the fabrication of an agar+gelatin+charcoal soft tissue phantom which can be probed and digitally examined for tissue disruption utilizing a biological image analysis script. An accurate mimic of soft tissue is paramount in importance as the according testing results must be accurately representative of real-life application of the probes. Agar-gelatin mixtures are commonplace in biological investigation of soft tissue characteristics because of its cheap, modular, and representative properties [27]. Agar provides necessary structural stability while gelatin offers a soft and elastic texture; the modularity of each of these components concentration allows for specific targeting of tissue types properties [28]. Necessary for application, a mimic adjacent to lacrimal soft tissue requires precise stiffness, with viscoelastic behavior and slow elastic recovery [29]. To achieve such properties, a mixture of 0.25% agar with 6% gelatin was utilized to generate the samples. Use of charcoal powder gives a stark contrast to the mixture and generates a dot-based scatter to systematically characterize the tissue sample within the Python algorithm. A more in-depth procedure of fabrication can be found in Appendix J.

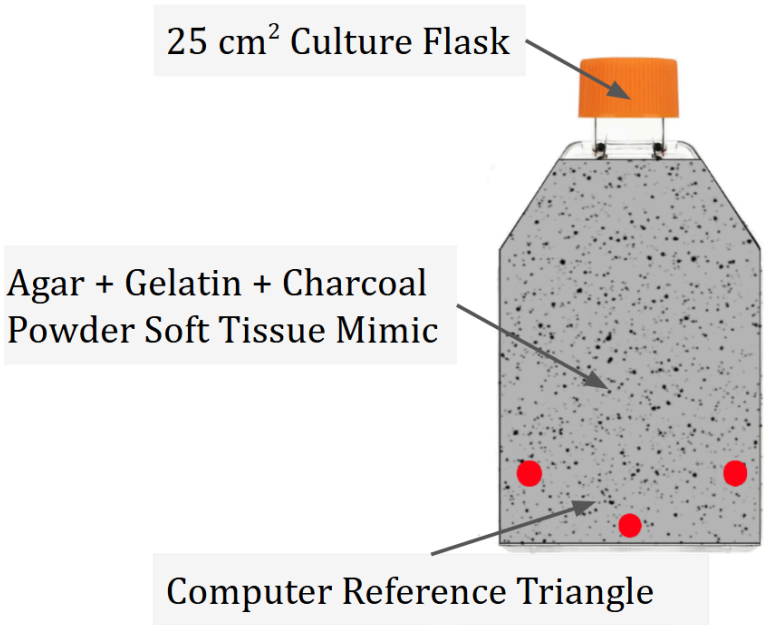

Figure 15: Tissue pull soft tissue mimic setup

Three trials of five different probe sizes; (1,2,4,7,8), both graduated and ungraduated, were performed on a set of five mimic samples. Before and after images of each individual trial were taken of the samples and ran through the Python script for acquisition of the percent change between the images. The script utilizes the same

binary image thresholding techniques deployed in magnetic resonance imaging (MRI) [30]. It first orients the before and after images exactly aligned using the designated colored anchors on the test samples. Once layered, the combined image is converted into a grey scale difference overlay of the pixel-specific variation between the images. If the pixels have undergone significant change between images, they are designated as white and those which remain the exact same are designated black, with everything in between designated along a monochrome spectrum. A region of interest (R.O.I.) is then applied which focuses the algorithm to analyze a single section of the image, the region which was probed. This region application helps to eliminate noise and localize a percent change to the probed region, making the resultant quantitative change more representative of the disruption induced by the probing itself. A threshold value is then utilized to partition the image binarily, helping distinguish actual change from extraneous alterations in appearance such as lighting and glare. This threshold assigns a color value between black, 0, and white, 255, as the value in which a pixel is officially evaluated to have changed or not. A threshold value of 133 was experimentally determined and defined in this experiment through analysis of noise influence and disruption visibility. The resulting image is a binary black and white photo where each white pixel is considered changed or disrupted and each black pixel considered the same. The image in general appears mostly black as the amount of change inflicted by the probe is minimal in even the most disruptive trials. Using this binary diagram, the algorithm then computes the percent change by taking the proportion of white pixels over total pixels. Using this process for each before and after photo of each trial, a set of data was gathered to quantitatively characterize the influence of the graduation on the amount of tissue pull.

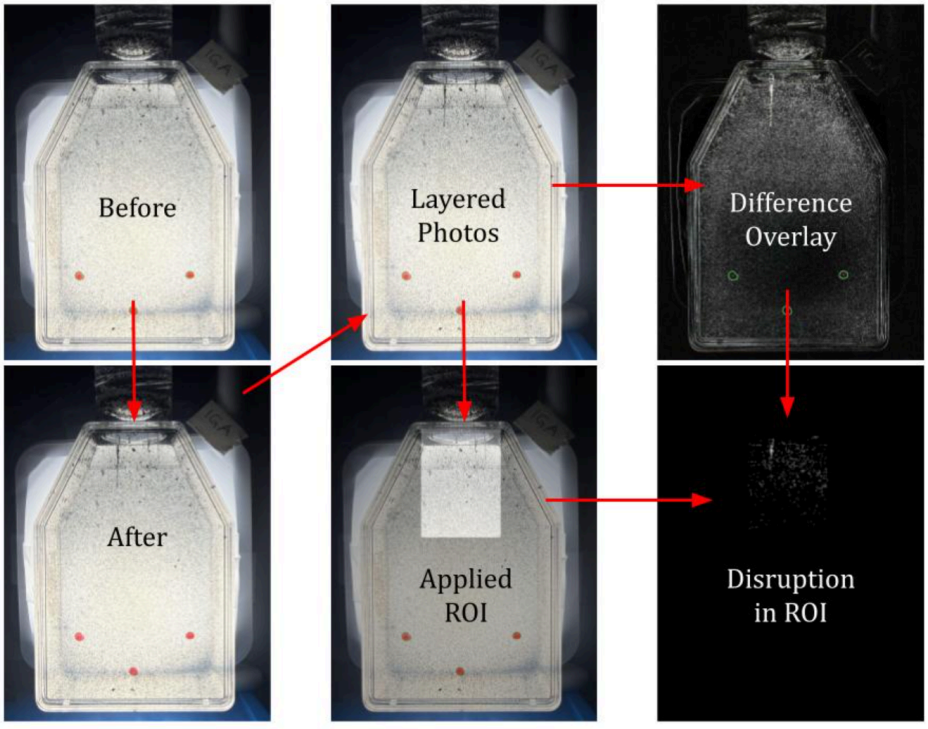

Figure 16: Figure representation of the logic flow used by the applied Python algorithm for determination of percent disruption induced by the probes.

Due to the independent and small nature of the samples, a test which utilizes mean difference to make inferences about similarity rather than identifying difference was deployed. Using a set of independent-sample TOST (two one-sided tests) with a delta value of 0.05 with n=3, and Welch degrees of freedom, a 90% confidence interval was generated and conclusions about the similarity of the probe type's disruptive influence can be made. Similar to the cadaveric testing, no literature value for acceptable probe percent disruption exists. Therefore, an estimated threshold value needs to be determined. Because of the small scale of the percent differences being returned, and leaving room for computer analysis error, the 0.05 delta value resulting in a 0.1 error interval was chosen. Probe sizes 4, 7, and 8 all provided equivalence, passing the TOST test, proving similarity in tissue disruption between the ungraduated and graduated probe types. Sizes 1 and 2 however failed to prove equivalency across probe types because of the large disparity in percent difference found in these smaller probe sizes. To verify these findings, two sample t-tests were also run for each size. Aligning with TOST, each of 4, 7, and 8 failed to reject the null hypothesis meaning there was no conclusive evidence of difference between the samples. Similarly, probe size 2 also proved congruent, providing statistical significance with a p-value less than 0.05, rejecting the null and proving the difference between the probe types was down to more than simply chance, indicating these graduated probes led to significant disruption in comparison to the ungraduated probes. The probe size 1 however, failed to reject the null, meaning it was not conclusive as to if the data could prove difference between the probe types.

Based on the analysis, it can be observed that the smaller probe sizes struggled with increased disruption across probe types in comparison to the larger probe sizes. Causes of this may include the graduation being marked differently because of the smaller diameter of the probe shafts, or an increased stress concentration due to a smaller cross sectional area contacting the tissue mimic. For this data in general, the extremely small sample size and variability brought in by the computer analysis necessitates further experimental testing with a larger pool of data to make robust conclusions about the state of graduated tissue pull. It is also imperative to consider that the agar-gelatin soft tissue mimic developed for this test is not a perfect representation of the true mechanical behavior of the lacrimal soft tissue. In order to develop keener insight into the graduates behavior, deeper investigation with a more finely curated phantom material is needed.

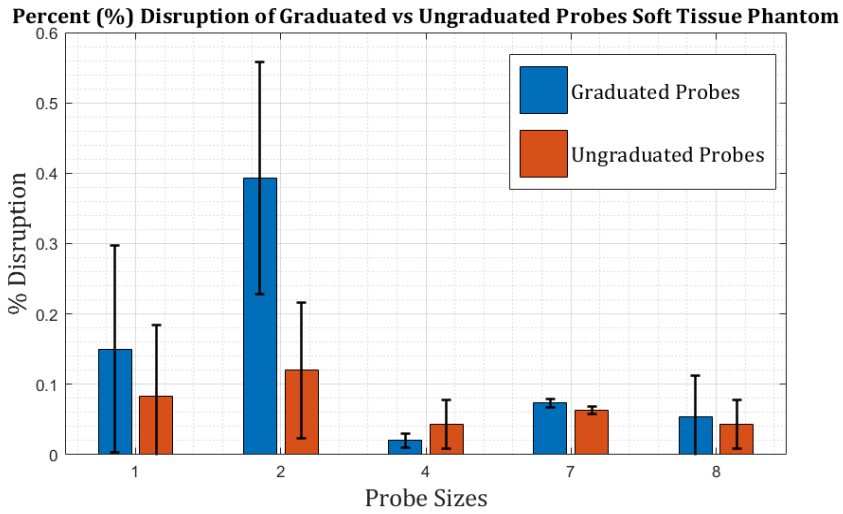

Figure 17: Comparison of graduated and ungraduated probes % disruption of an agar, gelatin and charcoal soft tissue phantom to display change in chance of tissue pull

C. Autoclave Testing

In order to fulfill necessary autoclave endurance parameters defined within the PDS, the fabricated probe must endure an extensive material deposition test to ensure the integrity of the probe's safety moving towards actual ophthalmological implementation. In the test, a control group, a set of regular commercial-grade probes and a test group, an associating set of fabricated graduated probes, were put through several rounds of one hour autoclave sterilization cycles. The before and after recorded probe masses will be tracked and compared between the control and test group and then statistically analyzed for significant difference. Any observable damage or impact, including to the graduation marks, that the testing environments generated on the probes will also be qualitatively tracked and evaluated. After completion of three autoclave cycles, the mean loss of probe weight was 1.02 +/- 1.62 milligrams. Further inspection of these samples after trials showed that there was no impact to the graduation. A paired t-test was then conducted with a reported value of 0.185 indicating that there is no statistically significant difference between the probes weight prior and after autoclaving. Since there was a small sample size, it is not possible to predict the probes degradation over further autoclave testing. A complete data set is available in Appendix G.

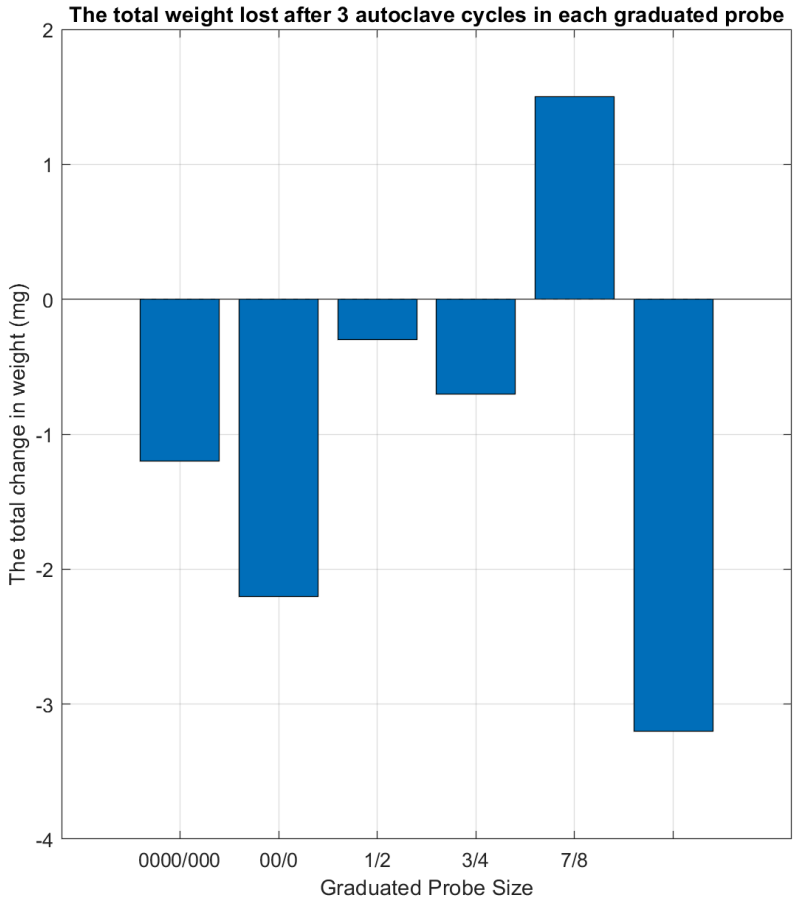

Figure 18: The graph represents the total weight change in milligrams after three autoclave cycles

D. Accelerated Life Testing

The graduated Bowman's probes must maintain their composition and procedural viability throughout the 5-10 year lifespan as stated by the client. To measure the potential visual degradation the probes will encounter while inside the lacrimal drainage system, an accelerated life test was conducted. Two pairs of probes of sizes 2 and 4, with one pair unmarked and the other graduated, were placed in artificial tear solution and kept in an InCu Safe incubator that maintained sterility, temperature at 37 ℃, and CO_2 levels at 5%. An in depth protocol for the preparation of the artificial tear solution is outlined in Appendix I. The probes were kept in the incubator for 48 hours, equating to 2,880 procedural uses, and then observed under a Leica MZ95 stereomicroscope to check for potential discoloration and marker degradation. While the probes had a slight discoloration, the markers remained distinguishable after accelerated life testing. It is important to note however, that this discoloration is uniform across both standard and graduated Bowman's probes, and that 2,880 procedural uses is uncommon as 2,000 is the typical lifespan of clinical probes.

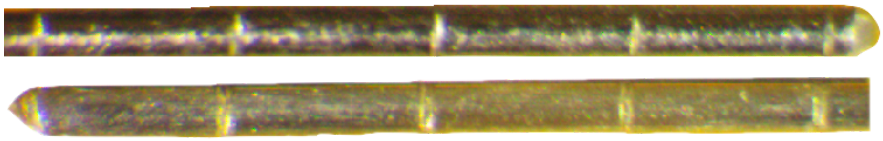

Figure 19: Top: Graduated Bowman probe, Bottom: Graduated Bowman probe after accelerated life testing

E. Uniformity Testing

In order to ensure the accuracy of probe markings and reproducibility of the graduated Bowman's probe's fabrication process, Uniformity testing was performed. 28 graduated probes of sizes ranging from 0000 to 7 were captured using a Leica MZ95 stereomicroscope. The position and magnification of the microscope were not changed in between images, allowing probes to be measured on the same scale. ImageJ was used to determine the interval length in between markings and marking widths. The distance from the end of the probe to the first marking was of particular importance, as it affects the accuracy of subsequent markings. After analyzing each probe, the average interval length was found to be 2.59 mm, corresponding to an average error of 3.71% from the target length of 2.5 mm, indicating strong consistency in spacing between markings. The average marking width was measured at 0.15 mm, with a higher average error of 15.35%; however, this variation is not practically significant, as it does not meaningfully affect the visibility of the markings. The average distance from the probe tip to the first marking was 2.78 mm. While this highlights an area where the fabrication process could be refined, it does not substantially impact the overall functionality of the probe. Collectively, these results demonstrate that the fabrication method produces probes with a high degree of reproducibility and sufficient accuracy for reliable clinical application. A complete data set is available in Appendix F.

F. Survey

Per client request, the graduated Bowman probe should not negatively alter current standard measurement procedures involving probe usage. In order to ensure that the fabricated design does not do so, a qualitative evaluation of the similarity and ease of use between procedure with a normal, commercial-grade probe and a fabricated, graduated probe was conducted. For this, Dr. Law and other medical school residents performed standard canalicular laceration depth estimates on cadaveric specimens with the graduated probe. They were then asked a series of questions about how the procedure went with the graduated probe, and if there were any significant ergonomic or procedural alterations that were made to routine operation as a result of the probe. A result of no procedural change will confirm the probe's theoretical implementation. All participants confirmed that during usage there was no change in technique required for the graduated probe. There was no concern of tissue pull and a professional opinion from Dr. Law stated that he preferred the graduated version over using a ruler to determine the depth due to the ease and efficiency of the process.

Discussion

The fabricated graduated Bowman probes succeeded in providing an alternative method to determine lacrimal measurements other than the standard ungraduated probe + ruler method. Quantitative and qualitative evaluation of the probes signified the potential that the probes contain for accurate diagnostic precision and ease of use. Due to the lack of graduated Bowman probes which not only don’t exist commercially but in general, a standard of quality does not exist to directly compare to. The graduated Bowman probe is a first of its kind and has real clinical potential. Fine tuning of fabrication and testing methods would help improve the probes consistency and would allow the generation of a representative quantitative characterization of the probes. The conducted survey of professional opinions backed the probe's design and preferred its simplicity to the current clinical standard.

A. Ethical Considerations

The biggest ethical consideration related to the graduated Bowman probes is its behavior during the procedure inside the body. After multiple different testing procedures to determine the compatibility of the design, the design itself will need to be submitted to the Institutional Review Board (IRB) for more detailed data acquisition in a controlled environment. The IRB will evaluate this design further to ensure ethical compliance and minimal risk to users. The important thing to note is that Bowman probes being used are already approved and used regularly in practice and the probes being modified will be the same. The addition of graduation through additive laser processing does not damage the integrity or change the mechanics of the probes, however, it is a new product and the changes should be considered. As mentioned by Dr. Law, if any risk is brought upon the patient from these probes, it would be due to error caused by the ophthalmologist performing the procedure. Since these probes have minimal mechanical change, the concern should be negligible.

B. Future Work

To further enhance the accuracy and ease of use for the graduated bowman probes, the interval lengths will be redesigned from every 2.5 mm to 1 mm. Every 5 mm, the marking associated will be darker, removing any potential error when counting markings. The current method for creating the markings is limited to a laser that is more advanced than necessary, requiring fabrication of a custom sample holder. Before these probes are to be used by ophthalmologists, further testing in live subjects is needed, as testing with cadavers does not account for biological variables present in the living tissues. These factors may influence the probe performance in unexpected ways, reducing the accuracy and safety that they demonstrated within cadavers. When these probes are to be implemented into hospitals, they would need to be more reproducible since their standard life in use is 5-10 years. For this to be possible, the fabrication protocol must account for all types of lasers and laser beds ensuring the same product is manufactured but with different materials.

Conclusions

The graduated Bowman’s probes were created to provide a more efficient and accurate method to measure the insertion depth of a probe in the lacrimal system, ultimately helping clinicians prescribe more personalized treatment plans for instances of nasolacrimal duct obstruction and canalicular laceration. As there are currently no graduated Bowman’s probes available on the market for clinical use, their creation and implementation is essential. The probe's final design features 2.5 mm interval markings from the tip up to 35 mm along the probe shaft. To manufacture the graduated Bowman probes, a laser fixture made of non-reflective aluminum was necessary to ensure focal point accuracy and manufacturing uniformity. The graduation markings were created using a LasX 200 Watt industrial laser that featured an additive process, ultimately maintaining the mechanical integrity of the original probes. Through qualitative and quantitative testing, the graduated prototypes were found to be a preferred, equivalently accurate method for lacrimal procedures in comparison to the medical standard, demonstrating substantial potential for real clinical improvement. However, with no medical-grade probes, minimal autoclave testing, and no living patient data, the graduated Bowman’s probe still requires further action. Surveyed residents had expressed the hope for smaller interval markings of 1mm in the future. The graduated Bowman’s probe should feature marker widths that are proportional to the size of the probe, and be manufactured using approved medical-grade 316L stainless steel. The manufactured prototypes must also be exposed to more cycles of tissue pull testing and autoclaving to have a holistic view of the prototypes lifespan. The proposed features and testing advancements, along with IRB approval, will allow for extended analysis of the graduated Bowman’s probes and will result in providing clinicians a faster and easier method of measurement acquisition.

References

any quantitative information without references came directly from the client, Dr. Law

[1] A. Pujari, M. S. Bajaj, and P. Sharma, “Calibrated Bowman’s lacrimal probe,” Indian journal of ophthalmology, https://pmc.ncbi.nlm.nih.gov/articles/PMC5859621/ (accessed Jan. 27, 2026).

[2] M. L. Cochran, S. Aslam, and C. N. Czyz, “Anatomy, Head and Neck: Eye Nasolacrimal,” in StatPearls, Treasure Island (FL): StatPearls Publishing, 2025. Accessed: Feb. 25, 2026. [Online]. Available: http://www.ncbi.nlm.nih.gov/books/NBK482213/

[3] R. R. A. Dantas, “Lacrimal Drainage System Obstruction,” Seminars in Ophthalmology, vol. 25, no. 3, pp. 98–103, May 2010, doi: 10.3109/08820538.2010.488577.

[4] C. L. Nicholas, “Fetal and neo-natal maxillary ontogeny in extant humans and the utility of prenatal maxillary morphology in predicting ancestral affiliation,” Am J Phys Anthropol, vol. 161, no. 3, pp. 448–455, Nov. 2016, doi: 10.1002/ajpa.23043.

[5] “Nasolacrimal Duct Disorders,” Riley Children’s Health. Accessed: Feb. 25, 2026. [Online]. Available: https://www.rileychildrens.org/health-info/nasolacrimal-duct-disorders

[6] Y. Perez, “Nasolacrimal duct obstruction,” StatPearls [Internet]., https://www.ncbi.nlm.nih.gov/books/NBK532873/ (accessed Jan. 27, 2026).

[7] “Eye Irritation: 8 Common Causes and How To Treat It.” Accessed: Feb. 25, 2026. [Online]. Available: https://my.clevelandclinic.org/health/symptoms/24607-eye-irritation

[8] M. Kothari, “Use of smart lacrimal probes,” Indian J Ophthalmol, vol. 59, no. 1, pp. 70–71, 2011, doi: 10.4103/0301-4738.73702.

[9] U. F. O. Themes, “Disorders of the Lacrimal System,” Ento Key. Accessed: Apr. 22, 2026. [Online]. Available: https://entokey.com/disorders-of-the-lacrimal-system-2/

[10] P. Phelps, “Canalicular laceration (trauma) - eyewiki,” American Academy of Ophthalmology - EyeWiki , https://eyewiki.org/Canalicular_Laceration_(Trauma) (accessed Apr. 29, 2026).

[11] R. Zhao et al., “Pediatric traumatic canalicular lacerations: Characteristics and prognostic factors,” Journal of ophthalmology, https://pmc.ncbi.nlm.nih.gov/articles/PMC12045685/ (accessed Apr. 29, 2026).

[12] M. L. Cochran, “Anatomy, head and neck: Eye Nasolacrimal,” StatPearls [Internet]., https://www.ncbi.nlm.nih.gov/books/NBK482213/#:~:text=Structure%20and%20Function,is%20the%20valve%20of%20Rosenmuller. (accessed Apr. 29, 2026).

[13] C. R. Rishor-Olney, “Canalicular laceration,” StatPearls [Internet]., https://www.ncbi.nlm.nih.gov/books/NBK560802/ (accessed Apr. 29, 2026).

[14] C.-H. Lin, C.-Y. Wang, Y.-C. Shen, and L.-C. Wei, “Clinical characteristics, intraoperative findings, and surgical outcomes of canalicular laceration repair with monocanalicular stent in Asia,” Journal of ophthalmology, https://pmc.ncbi.nlm.nih.gov/articles/PMC6636491/ (accessed Apr. 29, 2026).

[15] A. P. Murchison and J. R. Bilyk, “Canalicular Laceration Repair: An Analysis of Variables Affecting Success,” Ophthalmic Plastic & Reconstructive Surgery, vol. 30, no. 5, pp. 410–414, Sep. 2014, doi: 10.1097/IOP.0000000000000133

[16] I. O. Standardization, “ISO-13485:2016,” ISO, https://www.iso.org/obp/ui/en/#iso:std:iso:13485:ed-3:v1:en (accessed Feb. 4, 2026).

[17] D. F. Chang, N. Mamalis, and Ophthalmic Instrument Cleaning and Sterilization Task Force, “Guidelines for the cleaning and sterilization of intraocular surgical instruments,” Journal of Cataract and Refractive Surgery, vol. 44, no. 6, pp. 765–773, Jun. 2018, doi: https://doi.org/10.1016/j.jcrs.2018.05.001.

[18] Anthony Products, “Bowman lacrimal probes,” Anthony Products, https://anthonyproducts.com/bowman-lacrimal-probes (accessed Feb. 24, 2026).

[19] Laserax, “How Does Laser Annealing Work? | Laserax.” Accessed: Feb. 25, 2026. [Online]. Available: https://www.laserax.com/blog/how-does-laser-annealing-work

[20] E. C. Gugua, C. O. Ujah, C. O. Asadu, D. V. Von Kallon, and B. N. Ekwueme, “Electroplating in the modern era, improvements and challenges: A review,” Hybrid Advances, vol. 7, p. 100286, Dec. 2024, doi: 10.1016/j.hybadv.2024.100286.

[21] olikrom, “Intelligent pigments : A revolution in health and cosmetics,” OliKrom. Accessed: Feb. 25, 2026. [Online]. Available: https://www.olikrom.com/en/blog-olikrom/the-expert-eye/impact-of-color-change-materials-in-the-medical-industry/

[22] J. Jeffries, “Medical stainless steel maintenance and cleaning guide,” Infinium Medical, https://infiniummedical.com/medical-stainless-steel-maintenance-cleaning/ (accessed Jan. 28, 2026).

[23] Y. Xu et al., “A short review of medical-grade stainless steel: Corrosion resistance and novel techniques,” Science Direct, https://www.sciencedirect.com/science/article/pii/S2238785424002400?via%3Dihub (accessed Jan. 28, 2026)

[24] A. Schkutow and T. Frick, “Laser color marking of stainless steel – Investigation of the fluence-dependent and thermal mechanisms in generating laser induced surface modifications,” Procedia CIRP, vol. 124, pp. 661–664, Jan. 2024, doi: 10.1016/j.procir.2024.08.196.

[25] Jeremy, “When to Anneal Your Steel: Laser Annealing as an Alternative to Engraving,” RMI Laser. Accessed: Feb. 25, 2026. [Online]. Available: https://rmilaser.com/laser-annealing/

[26] Laserax, “How Does Laser Annealing Work? | Laserax.” Accessed: Feb. 25, 2026. [Online]. Available: https://www.laserax.com/blog/how-does-laser-annealing-work

[27] M. Navarro-Lozoya, M. S. Kennedy, D. Dean, and J. I. Rodriguez-Devora, “Development of Phantom Material that Resembles Compression Properties of Human Brain Tissue for Training Models,” Materialia (Oxf), vol. 8, p. 10.1016/j.mtla.2019.100438, Dec. 2019, doi: 10.1016/j.mtla.2019.100438.

[28] H. Yusuff, S. Chatelin, and J.-P. Dillenseger, “Narrative review of tissue-mimicking materials for MRI phantoms: Composition, fabrication, and relaxation properties,” Radiography, vol. 30, no. 6, pp. 1655–1668, Oct. 2024, doi: 10.1016/j.radi.2024.09.063.

[29] A. Maliborski and R. Różycki, “Diagnostic imaging of the nasolacrimal drainage system. Part I. Radiological anatomy of lacrimal pathways. Physiology of tear secretion and tear outflow,” Med Sci Monit, vol. 20, pp. 628–638, Apr. 2014, doi: 10.12659/MSM.890098.

[30] V. Vadmal, G. Junno, C. Badve, W. Huang, K. A. Waite, and J. S. Barnholtz-Sloan, “MRI image analysis methods and applications: an algorithmic perspective using brain tumors as an exemplar,” Neurooncol Adv, vol. 2, no. 1, p. vdaa049, Apr. 2020, doi: 10.1093/noajnl/vdaa049.

Appendix A: Product Design Specifications

Graduated Bowman Probe

BMEDesign: Product Design Specification

February 5, 2026

Biomedical Engineering 301

Section 304

Client: Dr. James Law & Dr. Suzanne van Landingham

Advisor: Prof. Monica Ohnsorg

Team Members:

Neel Srinivasan (Leader, BPAG) | nsrinivasan8@wisc.edu

Cole Miller (Communicator) | ctmiller8@wisc.edu

Caden Robinson (BSAC) | carobinson5@wisc.edu

Caleb White (BWIG) | cfwhite@wisc.edu

Function

Bowman probes are the standard instrument used in interrogation of the nasolacrimal (tear duct) system in Ophthalmology. They are available in various sizes and provide tactile feedback to the surgeon when probing the canalicular/nasolacrimal system, allowing them to assess for strictures, discontinuities, obstruction, or other abnormality within its lumen. Probing is typically performed prior to the passage of implants such as nasolacrimal stents (eg. Crawford, Lacriflow, Nunchucku, Monoka), to confirm patency of the nasolacrimal system. Available probes on the market do not have any markings on them which may allow the surgeon to make measurements to points within the canalicular/nasolacrimal lumen (eg. a stricture at 30 mm distal to the punctum), which can be helpful in correlating with imaging findings, or for accurate clinical documentation and therefore inform management of nasolacrimal pathologies. The development of such a stent with inscribed bands corresponding to millimeter markings will be essential during canalicular or nasolacrimal probing for the simple location of duct obstructions.

Client requirements

- The design must feature accurate line markings that are easily recognizable during procedures
- Device must be smooth and shouldn't have any engravings that result in a rough-textured surface
- The device's material must be compositionally strong after addition of measurement markers
- The design must be able to withstand autoclaving and repeated sterilization
- The design should fit standard probe size guidelines

Design requirements

1. **Physical and Operational Characteristics**

    a. **Performance requirements -** The device should be able to accurately present the depth of nasolacrimal duct probe insertion in millimeters. The device must be similar in comfort to the user's previous probes to avoid discomfort and procedural-change. The device must also be able to undergo multiple rounds of sterilization via autoclaving, and therefore must maintain structural and chemical integrity throughout high temperature exposure. Finally, the device must be able to withstand long-term usage without material degradation and/or mechanical failure.

    b. **Safety -** The selected design must comply with ISO-13485:2016 to uphold necessary safety and regulatory requirements[1]. This standard specifies the need for design risk assessment, product cleanliness, and overall quality assurance for medical devices. Should the design feature laser engraved measurement markings per the client's request, it must be tested and held to ISO-13485:2016 standards to ensure material composition and therefore patient safety is not jeopardized. Furthermore, the design's strength should be tested through MTS compression testing to confirm material integrity after the addition of measurement markers. While the procedure has minimal operating times, with the device being implanted for less than one minute, the design must follow ISO-10993-1 which specifies necessary guidelines for

biomaterial interactions with live tissue. A majority of design safety specifications are largely covered in sections 3a: Standards and Specifications and 3c: Patient Related Concerns.

c. **Accuracy and Reliability -** The design should have accurate markings every 5 mm along the probe as requested by the client, and feature inscribed bands corresponding to millimeter markings. The chosen device must also be within a normal range of standard commercial bowman probes in terms of weight, length, and diameter to comply with standard procedural operation. The measured values must be within a 5% range of the correct nasolacrimal duct obstruction millimeter length.

d. **Life in Service -** The design must be reusable, withstanding 5-10 years of clinical use. In order to achieve this, the probe should be designed from a material significantly resistant to wear and corrosion, such as stainless steel. This is particularly important for the design, since wearing down of the markings could harm functionality of the probe or lead to incorrect measurements In addition, the probes must be capable of withstanding hundreds of sterilization cycles, typically performed via autoclaving[2]. Individual uses of probes last from seconds to a minute.

e. **Operating Environmen**t - The design must be able to withstand all qualities of a clinical environment, as well as the environment of the tear duct. Firstly, the probe must be able to withstand temperatures of up to 132-135 °C to withstand the autoclaving process[2]. The probe will not be subjected to significant pressure, and will be exposed to the moderate humidity of operating rooms, ranging from 20-60% RH[3]. Additionally, the probe will be exposed to increased moisture during autoclaving. While being used, the probe will be exposed to the fluids of the tear duct, including tears, blood, and mucous. Particular care must be used to ensure probes are not contaminated between uses.

f. **Ergonomics -** The probe will be designed for use by trained clinical personnel and Ophthalmologists, who are familiar with bowman probes and how to handle clinical instruments. The probe must be designed to be comfortably and precisely controlled by gloved fingertips, typically achieved using a flat center. The probe must withstand minimal insertion force, up to 1 N[4], and the minimal torsion force caused by twisting. Fatigue is not a concern for this design, as they are intended to be used for a short duration. To ensure the safety of the patient, the probe should feature a rounded, atraumatic tip to prevent cutting. Finally, the design material should have a smooth, polished surface to prevent tissue trauma and improve tactile feedback. This extends to the graduated markings or engravings of the design.

g. **Size -** Bowman probes are available in sizes ranging from 0000-8. For the purposes of this project, the client is most concerned with sizes, 00, 0, and ½, representing 0.7 mm, 0.8mm and 1mm diameters, respectively. Additionally, probes are available in lengths ranging from 130-150mm. Finally, the probes come either curved or straight, however the client only uses straight probes.

h. **Weight -** These probes are typically very tiny and light to allow the ophthalmologist to be as precise as possible while performing the procedure to minimize error. Bowman probes weigh

roughly 45 grams. If this weight were to be increased by using different material, the probe would be more likely to cause error by puncturing the walls of the nasolacrimal cavities. If it were to be lighter, the probe's structural integrity could be more likely to fail during the procedure and further complicate the procedure.

i. **Materials -** Materials used to make probes must be organic metals that can be used in the body and minimize the risk of the patient creating some toxicity or allergy to it. The majority of the probes are made from stainless steel since the material combines strong structural integrity with flexibility [5]. The bowman probe must also be able to withstand sterilization techniques, the most prominent of which being the autoclave (temperatures range from 121 to 134 degrees C). Finally, the material must be smooth and blunt to, again, minimize injury. A semi-sphere will be attached to the end of the probe to remove any sharp edges that could cause damage to the patient.

j. **Aesthetics, Appearance, and Finish -** Probe will be thin, smooth, and be very forward looking about its usage. There should be no changes to probes already used in practice by ophthalmologists other than the changes to read measurements.

2. **Production Characteristics**

a. **Quantity -** As a preliminary approximation, 10 probes should be made for testing, allowing for multiple trials testing the integrity of the measurement tactics used. Allowing for multiple probes will provide a good baseline for techniques that work and those that don't. Although 10 is an approximation, it is likely that more will be used during testing especially because of the teams lack of training when applying these probes. Multiple errors could be made during fabrication assuming that a specific technique would be used and the probes are built accordingly, but in reality, medical professionals use another resulting in these probes to break.

b. **Target Product Cost -** The target product cost is $100 but can be changed depending on the progress made with the project. Depending on the materials used, the final product can be more expensive but the team will make it a priority to make the product as cost effective as possible. Most of the expense will most likely come from buying the actual probes to prototype on and test. When the device is fully functional, optimizations to the device will be made to further lower the cost to make it more widely available for anyone.

3. **Miscellaneous**

a. **Standards and Specifications**

i. ISO 10993-1 provides guidelines for toxicity testing of biomaterials in order to prepare for their interaction with living tissue. The evaluation is based on the specific materials used, how it contacts the body, and the duration of that contact. It provides an in-depth biological risk analysis, evaluation, and control procedure to allow for biocompatible confirmation of a material or device and is an internationally recognized biocompatibility assessment that is required for numerous regulatory applications [6]. The Bowman Probe

comes in direct contact with the lacrimal epithelium of the human body during operation and therefore falls under this guideline [7].

ii. ISO 13402:2025 describes specific test methods to evaluate the resistance of stainless steel surgical instruments from autoclaving, corrosion, and thermal exposure. It outlines procedures specific to typical alloy compositions with each individual test evaluating the materials effective resistance against each of the three aforementioned qualities. [8] The Bowman Probes used at the UW Hospital are sterilized via autoclave and must be corrosion-resistant to ensure long-term durability and to prevent alloy degradation and therefore should abide by this standard.

iii. ISO 17664 specifies the appropriate procedure for cleaning, disinfecting, and sterilizing medical devices. It describes the characteristics an appropriate medical device must have which includes being easy to clean and sterilize as well as an associating proof of sterilization through formalized testing and data collection. It breaks down medical devices into three categories, critical, semi-critical, and non-critical, with surgical tools being deemed critical and therefore requiring the most attention as they pose the highest risk of infection [9]. Bowman probes are categorized as a surgical tool due to their vital role in ophthalmological procedure and therefore require high sterilization efforts.

iv. ASTM B912 specifies the passivation of stainless steel alloys through electropolishing. It gives a detailed outline for the pre-treatment, electropolishing, and post-electropolishing processes for various grades of stainless steel [10]. The Bowman Probes will be manufactured out of stainless steel and will require a surface restoration process following any modifications made to the probe in order to prevent alloy deposition and an associating inflammatory response [11].

v. 21 CFR Part 820 is a quality system regulation standard for medical devices which provides necessary details on the designing, manufacturing, storage, and application of medical devices specific for human use. The criteria for this standard lie in tandem with the FDA and therefore provide a good basis for qualification of an appropriate medical device [12]. This standard could become extremely important for the graduated Bowman Probe depending on the extent of development that is done within the project sphere.

b. **Customer**

i. The users of the device will be Dr. James Law and Dr. Sarah van Landingham as well as other clinical practitioners in the ophthalmology department at the UW Hospital. They desire the implementation of the device to be a seamless process that swaps the current Bowman Probes for the modified devices, where no alteration to the methodology or step-wise process of the operation is required.

ii. The probe will first be implemented into regular use at the UW Hospital and can eventually further be placed on the market if the team identifies market potential.

c. **Patient-related concerns**

i. For medical patients whose operation will be completed with the modified device, all relevant concerns with the procedure both relating to and not relating to the modified Bowman Probe will have been approved and cleared by numerous medical professionals prior to the operation [13]. This includes all anesthetic, pain-related and biological safety concerns for the procedure. The device will be sterilized with an autoclave prior to and after each use and therefore must be tested for continued autoclave sterilization with no signs of damage or degradation.

ii. Potential exposure of alloy particulates to the epithelial-lined conduit of the nasolacrimal duct from laser engraving could cause an unintended inflammatory response within the eye and long term development of scar tissue [14]. The probe must undergo a surface restoration process in order to prevent this response from occurring, such as electropolishing. [15]. The graduated probes will be implemented into the congenital nasolacrimal duct obstruction procedure. This process involves perforating a thin epithelial membrane and is a relatively brief and concise operation, approximately 1 minute in total invasive time for adult patients . This brevity decreases the opportunity of particle deposition from these engravings and prevents intense chemical breakdown from the moist, protein rich environment of lacrimal mucosa [16].

iii. Because of the generation of microscopic burrs and sharp edges during the engraving process, there is an increased chance of prominent friction between the probe edge and the epithelial lining it contacts [16]. Since lacrimal epithelium is thin and delicate, there is potential for abrasion and damage to the surrounding tissue [17]. Thus, damage to the lacrimal tissue within the duct leading to small scale hemorrhage and the development of scar tissue within the lining, further closing the duct, poses a potential concern [18]. Similar to alloy deposition, surface restoration processes such as electropolishing are necessary to diminish the probability of this occurring.

d. **Competition**

Sklar Surgical Instruments

i. Sklar Bowman Probes are the most monetarily prolific brand in the market, bought in bulk by hospitals and other medical facilities [19]. They are known for reliability and quality and offer probe customization with various sizes and material options including stainless steel and silver [20].

ii. The probes are thin malleable rods with a rounded end used for clearing of the nasolacrimal duct, as well as other general procedures involving the lacrimal system. The device is double ended with distinct probe sizes on each end of a singular instrument.

iii. All probes offered by Sklar are bought non-sterile, reusable, and absent of any latex material helping prevent common anaphylaxis [20]. They are not graduated and therefore though medically acceptable, are not as quantitatively precise as desired by the client.

iv. A single Sklar Probe costs approximately 120 USD which stands at a higher end market price and quality.

Calibrated Bowman's lacrimal probe from Indian journal of ophthalmology.

i. These Bowman Probes were individually manufactured with numbered engraving to improve the diagnostic and therapeutic utility of the Bowman Probe in relevant ophthalmological procedures. The numbers have been engraved on the millimeter scale on either side of the probe using laser engraving [21].

ii. The graduated probes are made of stainless steel and feature the exact same size range as standard probes. They are double sided, contain a central metal plate for grip, and are reusable and sterilizable.

iii. The engravings provide nominal size references rather than specific discrete measurement points. The markings provide general guides for the distance of probe insertion into the lacrimal duct but no high level specificity.

iv. These probes are not commercially available and therefore cannot be monetarily purchased.

References

any quantitative information without references came directly from the client, Dr. Law

[1] I. O. Standardization, “ISO-13485:2016,” ISO, https://www.iso.org/obp/ui/en/#iso:std:iso:13485:ed-3:v1:en (accessed Feb. 4, 2026).

[2] D. F. Chang, N. Mamalis, and Ophthalmic Instrument Cleaning and Sterilization Task Force, “Guidelines for the cleaning and sterilization of intraocular surgical instruments,” Journal of Cataract and Refractive Surgery, vol. 44, no. 6, pp. 765–773, Jun. 2018, doi: https://doi.org/10.1016/j.jcrs.2018.05.001.

[3]“Guidelines for Best Practices for Humidity in the Operating Room,” 2015. Available: https://www.ast.org/uploadedFiles/Main_Site/Content/About_Us/ASTGuidelinesHumidityintheOR.pdf

[4] A. K. Golahmadi, D. Z. Khan, G. P. Mylonas, and H. J. Marcus, “Tool-tissue forces in surgery: A systematic review,” Annals of Medicine and Surgery, vol. 65, p. 102268, May 2021, doi: https://doi.org/10.1016/j.amsu.2021.102268.

[5] “Bowman Lacrimal Probe,” Grey Medical. Accessed: Feb. 05, 2026. [Online]. Available: https://grey-medical.com/product/bowman-lacrimal-probe.html

[6] “ISO 10993-1:2025,” ISO. Accessed: Feb. 04, 2026. [Online]. Available: https://www.iso.org/standard/10993-1

[7] “Double Ended Ophthalmic Bowman Lacrimal Passage Probe.” Accessed: Feb. 05, 2026. [Online]. Available: https://www.surgical-tool.com/bowman-lacrimal-passage-probe/

[8] “ISO 13402:2025(en), Surgical and dental hand instruments — Determination of resistance against autoclaving, corrosion and thermal exposure.” Accessed: Feb. 04, 2026. [Online]. Available: https://www.iso.org/obp/ui/en/#iso:std:iso:13402:ed-2:v1:en

[9] “ISO 17664: Medical Device Cleaning Standards | SafetyCulture.” Accessed: Feb. 04, 2026. [Online]. Available: https://safetyculture.com/topics/iso/iso-17664

[10] “ASTM B912-02(2013) - Standard Specification for Passivation of Stainless Steels Using Electropolishing.” Accessed: Feb. 04, 2026. [Online]. Available: https://webstore.ansi.org/standards/astm/ASTMB912022013

[11] “Why Stainless Steel is the Preferred Material for Surgical Instruments | Applied Physics Medical.” Accessed: Feb. 05, 2026. [Online]. Available: https://appliedphysicsmedical.com/blog/durable-materials-surgical-instruments-stainless-steel

[12] “21 CFR Part 820 -- Quality System Regulation.” Accessed: Feb. 04, 2026. [Online]. Available: https://www.ecfr.gov/current/title-21/part-820

[13] “Tool and Resources.” Accessed: Feb. 04, 2026. [Online]. Available: https://www.who.int/teams/integrated-health-services/patient-safety/research/safe-surgery/tool-and-resources

[14] Y. Xu, Y. Li, T. Chen, C. Dong, K. Zhang, and X. Bao, “A short review of medical-grade stainless steel: Corrosion resistance and novel techniques,” Journal of Materials Research and Technology, vol. 29, pp. 2788–2798, Mar. 2024, doi: 10.1016/j.jmrt.2024.01.240.

[15] J. A. Sandoval-Robles, C. A. Rodríguez, and E. García-López, “Laser Surface Texturing and Electropolishing of CoCr and Ti6Al4V-ELI Alloys for Biomedical Applications,” Materials (Basel), vol. 13, no. 22, p. 5203, Nov. 2020, doi: 10.3390/ma13225203.

[16] “Lacrimal gland,” Kenhub. Accessed: Feb. 04, 2026. [Online]. Available: https://www.kenhub.com/en/library/anatomy/lacrimal-gland

[17] “Nasolacrimal duct,” Kenhub. Accessed: Feb. 05, 2026. [Online]. Available: https://www.kenhub.com/en/library/anatomy/nasolacrimal-duct

[18] “Blocked Tear Duct: Causes, Symptoms, Treatment & Prevention,” Cleveland Clinic. Accessed: Feb. 05, 2026. [Online]. Available: https://my.clevelandclinic.org/health/diseases/17260-blocked-tear-duct-nasolacrimal-duct-obstruction

[19] “Bowman Lacrimal Probe Industry Overview and Projections.” Accessed: Jan. 28, 2026. [Online]. Available: https://www.datainsightsmarket.com/reports/bowman-lacrimal-probe-1755038

[20] “Sklar Corporation,” Sklar Surgical Equipment. Accessed: Feb. 05, 2026. [Online]. Available: https://www.sklarcorp.com/

[21] A. Pujari, M. S. Bajaj, and P. Sharma, “Calibrated Bowman’s lacrimal probe,” Indian journal of ophthalmology, https://pmc.ncbi.nlm.nih.gov/articles/PMC5859621/ (accessed Jan. 27, 2026).

Appendix B: Expense Sheet

Item	Description	Manufacturer	Part Number	Date	QTY	Cost Each	Total	Link
Component 1								
Set of Bowman's probes	A set of unmarked Bowman's probes used in duct procedures for the team to practice fabrication and testing	Premium Instrument	B0777N38SV	2/25/26	3	$16.99	$50.97	Link
Component 2								
CerMark 2 oz Aerosol Ultra	A 2 oz aerosol can of CerMark ULTRA Aerosol spray used for laser marking of various materials including metals and ceramics.	CerMark USA	CULTRA.A2	3/11/2026	1	$17.00	$17.00	Link
LMM6018 CerMark USA white sheet tape tape	A small 2"x6" sheet of white tape used for laser marking definition on typically metal surfaces.	CerMark USA	CLMM6018.SH2	3/11/2026	1	$8.00	$8.00	Link
Component 3								
9.54mm x 76.09 x 115 mm Aluminum 6061	Non reflective aluminum used for laser fixture fabrication	ECB Stock Room	N/A	4/10/26	1	~$5.57	$5.57	N/A
TOTAL:	**$81.54**							

Appendix C: Tissue Pull Testing Python Code

```
import cv2
import numpy as np
import os
from scipy.spatial.distance import cdist
from skimage.exposure import match_histograms

# === SETUP ===
# Debugging flags
DEBUG_ANCHORS = False # turn on if you want to check if the mask is correctly isolating the
red Sharpie anchors
DEBUG_ROI = False # turn on if you want to visualize the ROI overlay and masked difference
THRESH_VIEW = False # turn on if you want to use threshold slider for tuning
ROI_FINDER = False # turn on if you want to use the ROI finder tool to set the ROI
coordinates

# File paths
BEFORE_FILE = '/Users/cfwhite/Downloads/bowman probe testing images/4GC_b.jpeg'
AFTER_FILE  = '/Users/cfwhite/Downloads/bowman probe testing images/4GC_a.jpeg'

# Region of Interest (ROI) Mask parameters: want it in probing area
ROI_X1, ROI_Y1 = 986, 13
ROI_X2, ROI_Y2 = 2486, 1913
# remember to maintain area across all runs

# global variables for ROI finder
ROI_W, ROI_H = 1500, 1900
roi_x, roi_y = 700, 100    # Initial starting position
dragging = False


# === FUNCTIONS ===
# ROI set up
def draw_roi(img, x, y):
    """
    Draws a rectangle representing the ROI on the image, along with
    text displaying the current coordinates of the ROI. It is used
    to interactively visualize and adjust the ROI position when
    using the ROI finder tool.

    Args:
        img: The input image on which to draw the ROI.
        x: The x-coordinate of the top-left corner of the ROI.
        y: The y-coordinate of the top-left corner of the ROI.

    Returns:
        An image with the ROI rectangle and coordinate text drawn on it.
    """
    temp_img = img.copy()
    # Draw ROI rectangle
```

```
    cv2.rectangle(temp_img, (x, y), (x + ROI_W, y + ROI_H), (0, 255, 0), 3)
    # Add info text
    text = f"ROI: X1={x}, Y1={y}, X2={x+ROI_W}, Y2={y+ROI_H}"
    font = cv2.FONT_HERSHEY_SIMPLEX
    font_scale = 3
    thickness = 6
    text_pos = (20, 100)

    (text_width, text_height), baseline = cv2.getTextSize(text, font, font_scale, thickness)
    cv2.rectangle(temp_img,
                  (text_pos[0], text_pos[1] - text_height - baseline),
                  (text_pos[0] + text_width, text_pos[1] + baseline),
                  (0, 0, 0),
                  -1)
    cv2.putText(temp_img, text, text_pos, font, font_scale, (255, 255, 255), thickness)
    return temp_img

def mouse_callback(event, x, y):
    """
    Handles mouse events for the interactive ROI finder tool. It allows
    the user to click and drag a rectangle on the image to set the
    desired ROI coordinates. When the user releases the mouse button,
    it updates the global ROI coordinates based on the final position
    of the rectangle.

    Args:
        event: The type of mouse event (e.g., button down, mouse move, button up).
        x: The x-coordinate of the mouse event.
        y: The y-coordinate of the mouse event.

    Modifies:
        Updates the global variables ROI_X1, ROI_Y1, ROI_X2, ROI_Y2 with the new
        ROI coordinates when the mouse button is released.
    """
    global roi_x, roi_y, dragging, ROI_X1, ROI_Y1, ROI_X2, ROI_Y2

    if event == cv2.EVENT_LBUTTONDOWN:
        # Check if click is inside the rectangle
        if roi_x <= x <= roi_x + ROI_W and roi_y <= y <= roi_y + ROI_H:
            dragging = True

    elif event == cv2.EVENT_MOUSEMOVE:
        if dragging:
            roi_x, roi_y = x - (ROI_W // 2), y - (ROI_H // 2)

    elif event == cv2.EVENT_LBUTTONUP:
        dragging = False
        ROI_X1 = roi_x
        ROI_Y1 = roi_y
        ROI_X2 = roi_x + ROI_W
        ROI_Y2 = roi_y + ROI_H
```

```
        print(f"Current ROI Coordinates: X1={ROI_X1}, Y1={ROI_Y1}, X2={ROI_X2},
Y2={ROI_Y2}")

# detect the red Sharpie anchors and return their centers and contours for shape matching
def detect_anchors(image):
    """
    Detects the red Sharpie anchors in the given image by applying color
    thresholding in the HSV color space, followed by contour detection.

    Args:
        image: The input image in which to detect the anchors.

    Returns:
        A tuple containing:
        - sorted_anchors: A list of contours corresponding to the
          detected anchors, sorted by area.
        - scale: The scaling factor used to resize the image for processing.
    """
    scale = 0.5
    small_img = cv2.resize(image, (0,0), fx=scale, fy=scale)

    denoised = cv2.medianBlur(small_img, 7) # use median blur to reduce noise
    hsv = cv2.cvtColor(denoised, cv2.COLOR_BGR2HSV)

    # define ranges for red (the red Sharpie)
    lower_red1 = np.array([0, 70, 50]) #([0, 150, 30])
    upper_red1 = np.array([10, 255, 255]) #([10, 255, 255])
    lower_red2 = np.array([170, 70, 50]) #([170, 150, 30])
    upper_red2 = np.array([180, 255, 255]) #([180, 255, 255])

    mask1 = cv2.inRange(hsv, lower_red1, upper_red1)
    mask2 = cv2.inRange(hsv, lower_red2, upper_red2)
    mask = cv2.bitwise_or(mask1, mask2) # bitwise is used for binary mask (black and white)

    kernel = cv2.getStructuringElement(cv2.MORPH_ELLIPSE, (5, 5))
    mask = cv2.morphologyEx(mask, cv2.MORPH_OPEN, kernel)
    mask = cv2.morphologyEx(mask, cv2.MORPH_CLOSE, kernel)

    contours, _ = cv2.findContours(mask, cv2.RETR_EXTERNAL, cv2.CHAIN_APPROX_SIMPLE)

    min_area = 100
    # valid_contours = [cnt for cnt in contours if cv2.contourArea(cnt) > min_area]
    valid_contours = []

    for cnt in contours:
        area = cv2.contourArea(cnt)
        if area < min_area:
            # Draw tiny ones as red or skip them entirely
            continue

        perimeter = cv2.arcLength(cnt, True)
```

```
        if perimeter == 0:
            continue

        # Calculate properties
        circ = 4 * np.pi * area / (perimeter ** 2)
        x, y, w, h = cv2.boundingRect(cnt)
        aspect_ratio = w / float(h)
        extent = area / (w * h)
        hull = cv2.convexHull(cnt)
        hull_area = cv2.contourArea(hull)
        solidity = area / hull_area if hull_area > 0 else 0

        # Apply your logic (Loosen these as needed)
        if (
            circ > 0.4 and
            0.5 < aspect_ratio < 2.0 and
            extent > 0.3 and
            solidity > 0.7
        ):
            valid_contours.append(cnt)
            # DRAW GREEN for VALID
            cv2.drawContours(small_img, [cnt], -1, (0, 255, 0), 2)
        else:
            # DRAW RED for REJECTED (This helps you see what is failing!)
            cv2.drawContours(small_img, [cnt], -1, (0, 0, 255), 2)
            # Optional: print properties to console for debugging
            # print(f"Rejected: Circ={circ:.2f}, Aspect={aspect_ratio:.2f},
Solidity={solidity:.2f}")

    if len(valid_contours) < 3:
        all_areas = sorted([cv2.contourArea(c) for c in contours], reverse=True)
        #raise ValueError(f"Found only {len(valid_contours)} anchors. Contour areas found:
{all_areas}")

    # Find centers of the anchors
    centers = []
    sorted_anchors = sorted(valid_contours, key=cv2.contourArea, reverse=True)[:3]

    for cnt in sorted_anchors:
        M = cv2.moments(cnt)
        if M["m00"] != 0:
            cX = int(M["m10"] / M["m00"])
            cY = int(M["m01"] / M["m00"])
            centers.append((cX / scale, cY / scale))

    return sorted_anchors, centers, scale, mask, small_img

# Sort points consistently (set up for affine transformation):
# places the three points of the triangle in a consistent order (top, bottom-left,
bottom-right) across both images
def sort_triangle_points(pts):
```

```
    """
    Sorts the three points of the triangle in a consistent order: top,
    bottom-left, bottom-right.

    Args:
        pts: An array of shape (3, 2) containing the (x, y) coordinates
        of the three points.

    Returns:
        An array of shape (3, 2) with the points sorted in the order:
        [top_point, bottom_left_point, bottom_right_point]
    """
    # sort by y (top vs bottom)
    pts = np.array(pts)

    # Peak = point with largest y (lowest in image)
    peak_idx = np.argmax(pts[:,1])
    peak = pts[peak_idx]

    # Remaining two are base
    base = np.delete(pts, peak_idx, axis=0)

    # Sort base left → right
    base = base[np.argsort(base[:,0])]

    return np.array([base[0], base[1], peak])

def calculate_roi(pts, img_shape, roi_w=900, roi_h=1225):
    """
    Calculates the ROI coordinates based on the center of the three
    anchor points.

    Args:
        pts: An array of shape (3, 2) containing the (x, y) coordinates of the three anchor
points.
        img_shape: A tuple containing the shape of the image (height, width).
        roi_w: The width of the ROI box.
        roi_h: The height of the ROI box.

    Returns:
        A tuple containing the ROI coordinates (roi_x1, roi_y1, roi_x2, roi_y2)
    """
    center_x = int(np.mean(pts[:, 0])) # find the center of all anchors

    ### CHANGE
    y1 = 725 # fixed 800: 1, and 7 probes
    # 900: 2
    # 1225: 8
    # 725: 4

    y2 = roi_h + y1 # Box height goes from 0 to 1900
```

```
    # find X range based on the center
    x1 = center_x - (roi_w // 2)
    x2 = center_x + (roi_w // 2)

    # check that ROI box doesn't go off-screen
    roi_x1 = max(0, x1)
    roi_x2 = min(img_shape[1], x2)

    return roi_x1, y1, roi_x2, y2

def draw_anchors(img, contours, scale):
    """
    img: The original resolution image
    contours: The list of contours detected in the scaled-down image
    scale: The scale factor (0.5)
    """
    # Scale the contours up to original size by creating a new list
    # where every coordinate (x, y) is divided by the scale
    scaled_contours = [ (cnt / scale).astype(int) for cnt in contours ]

    # Draw the contours (anchors)
    # -1 draws all contours, (0, 255, 0) is green, 2 is thickness
    cv2.drawContours(img, scaled_contours, -1, (0, 255, 0), 2)

    # Draw the centers of the anchors
    for cnt in scaled_contours:
        M = cv2.moments(cnt)
        if M["m00"] != 0:
            cX = int(M["m10"] / M["m00"])
            cY = int(M["m01"] / M["m00"])
            # Draw a red dot at the center
            cv2.circle(img, (cX, cY), 7, (0, 0, 255), -1)


# === PIPELINE: load images, detect circles, find triangle, align images, apply ROI mask,
analyze
# --- Load images ---
before = cv2.imread(BEFORE_FILE)
after  = cv2.imread(AFTER_FILE)

if ROI_FINDER:
    # Choose if you want to enter values or use the ROI finder tool
    print("Press 1 to enter ROI coordinates manually, or 2 to use the interactive ROI finder
tool.")
    choice = input("Enter your choice (1 or 2): ")
    if choice == '1':
        ROI_X1 = int(input("Enter ROI X1: "))
        ROI_Y1 = int(input("Enter ROI Y1: "))
        ROI_X2 = int(input("Enter ROI X2: "))
        ROI_Y2 = int(input("Enter ROI Y2: "))
```

```
        print(f"ROI set to: X1={ROI_X1}, Y1={ROI_Y1}, X2={ROI_X2}, Y2={ROI_Y2}")
    elif choice == '2':
        cv2.namedWindow("ROI Tuner", cv2.WINDOW_NORMAL)
        cv2.setMouseCallback("ROI Tuner", mouse_callback)

        print("Drag the rectangle to position the ROI. Press 'q' to exit.")

        while True:
            display_img = draw_roi(before, roi_x, roi_y)
            cv2.imshow("ROI Tuner", display_img)
            if cv2.waitKey(1) & 0xFF == ord('q'):
                break

        cv2.destroyAllWindows()

# Detect contours
before_contours, before_centers, before_scale, before_mask, _ = detect_anchors(before)
after_contours, after_centers, after_scale, after_mask, _ = detect_anchors(after)
#matched_pairs = match_anchors(before_contours, after_contours) # match based on shape
identity

if DEBUG_ANCHORS:
        # Stack masks side by side
        mask_combined = np.hstack((before_mask, after_mask))

        # Convert masks to color to overlay contours
        before_overlay = cv2.cvtColor(before_mask, cv2.COLOR_GRAY2BGR)
        after_overlay  = cv2.cvtColor(after_mask, cv2.COLOR_GRAY2BGR)

        cv2.drawContours(before_overlay, before_contours, -1, (0,255,0), 2)
        cv2.drawContours(after_overlay, after_contours, -1, (0,255,0), 2)

        overlay_combined = np.hstack((before_overlay, after_overlay))

        cv2.imshow("MASKS: Before | After", mask_combined)
        cv2.imshow("VALID CONTOURS: Before | After", overlay_combined)

        cv2.waitKey(0)

'''
# extract centers for the affine transformation ONLY if they are the correct pairs
before_pts = []
after_pts = []

for b_cnt, a_cnt in matched_pairs:
    # get centers from before image
    M_b = cv2.moments(b_cnt)
    b_cx = int(M_b["m10"] / M_b["m00"])
    b_cy = int(M_b["m01"] / M_b["m00"])
    before_pts.append([b_cx / scale, b_cy / scale])
```

```
    # get centers from after image
    M_a = cv2.moments(a_cnt)
    a_cx = int(M_a["m10"] / M_a["m00"])
    a_cy = int(M_a["m01"] / M_a["m00"])
    after_pts.append([a_cx / scale, a_cy / scale])
'''
#before_pts = np.array(before_pts, dtype=np.float32)
#after_pts = np.array(after_pts, dtype=np.float32)
if len(before_centers) != 3 or len(after_centers) < 3:
    print(f"CRITICAL ERROR: Detection failed.")
    print(f"Found in Before: {len(before_centers)} anchors")
    print(f"Found in After: {len(after_centers)} anchors")
    raise ValueError("Could not find 3 anchors in one or both images. Check your
lighting/thresholds.")
before_pts = sort_triangle_points(before_centers)
after_pts = sort_triangle_points(after_centers)

# Use anchor points to choose the ROI dynamically
ROI_X1, ROI_Y1, ROI_X2, ROI_Y2 = calculate_roi(before_pts, before.shape[:2])

# Compute affine transform: maps the three points from the "after" image to the
# corresponding points in the "before" image
M, _ = cv2.estimateAffinePartial2D(after_pts, before_pts) # returns a tuple (matrix,
inliers) so take [0] to get the matrix

# Align images using the computed affine transformation
aligned_after = cv2.warpAffine(after, M, (before.shape[1], before.shape[0]))

# --- Analyze differences ---
diff = cv2.absdiff(before, aligned_after) # calculates absolute difference between before
and after
gray_diff = cv2.cvtColor(diff, cv2.COLOR_BGR2GRAY) # change image to black and white
_, thresh = cv2.threshold(gray_diff, 110, 255, cv2.THRESH_BINARY) # sensitivity threshold
# if pixel intensity is < 30, change it to black (0)
# if pixel instensity is >= 30, set it to white (255)

# ROI Masking
roi_mask = np.zeros(diff.shape[:2], dtype=np.uint8)
cv2.rectangle(roi_mask, (ROI_X1, ROI_Y1), (ROI_X2, ROI_Y2), 255, -1) # create mask
masked_diff = cv2.bitwise_and(thresh, thresh, mask=roi_mask) # apply mask

# Metrics using ROI
change_pixel_count = cv2.countNonZero(masked_diff)
total_pixels = cv2.countNonZero(roi_mask) # denominator

if total_pixels > 0:
    percentage_change = (change_pixel_count / total_pixels) * 100
    print(f"File: {os.path.basename(BEFORE_FILE)}")
    print(f"Percentage of changed pixels: {percentage_change:.2f}%")
else:
    print("ROI has zero pixels, cannot compute percentage change.")
```

```
# Visualize anchors
draw_anchors(before, before_contours, before_scale)
draw_anchors(after, after_contours, after_scale)
draw_anchors(diff, before_contours, before_scale)
draw_anchors(diff, after_contours, after_scale)

# --- Show results ---
cv2.imshow("Before", before)
cv2.imshow("After", after)
cv2.imshow("After (aligned)", aligned_after)
cv2.imshow("Difference", diff)
cv2.imshow("Thresholded Change", thresh)

'''# --- Download Results ---
cv2.imwrite('before.jpg', before)
cv2.imwrite('after.jpg', after)
cv2.imwrite('aligned_after.jpg', aligned_after)
cv2.imwrite('diff.jpg', diff)
cv2.imwrite('masked_diff.jpg', masked_diff)'''

if DEBUG_ROI:
    # Overlay ROI for debugging
    debug_view = cv2.addWeighted(before, 0.7, cv2.cvtColor(roi_mask, cv2.COLOR_GRAY2BGR),
0.3, 0) # ROI debug view
    cv2.imshow("ROI Debug View", debug_view)
    cv2.imwrite('roi_debug_view.jpg', debug_view)
cv2.imshow("Difference in ROI", masked_diff)

if THRESH_VIEW:
    def nothing(x): pass
    cv2.namedWindow("Threshold Tuning")
    cv2.createTrackbar("Threshold", "Threshold Tuning", 70, 255, nothing)

    while True:
        thresh_value = cv2.getTrackbarPos("Threshold", "Threshold Tuning")
        _, thresh_img = cv2.threshold(gray_diff, thresh_value, 255, cv2.THRESH_BINARY)
        cv2.imshow("Threshold Tuning", thresh_img)
        if cv2.waitKey(1) & 0xFF == ord('q'):
            break

cv2.waitKey(0)
cv2.destroyAllWindows()
```

Appendix D: Cadaveric Testing Raw Test Data and MATLAB Code

Station #	Estimated (no measurements) (mm)	Bowman probe + No Ruler (mm)	Bowman Probe + Ruler (Gold Standard) (Actual) (mm)	Graduated Bowman Probe (mm)
1L (Lower)	5	5	5	5
1R (Upper)	2	3	3	2.5
2L(Lower)	1.5	1.5	2	1.25
2R(Upper)	15	3	3	3
3L(Lower)	2	2	2	2
3R(Upper)	2.5	3	3	3
4L(Lower)	8	8	8	7.5
4R(Upper)	15	15	14	14
5L(Lower)	0	0	0	0
5R(Upper)	10	12	11	11

Resident 1

Station #	Estimated (no measurements)	Bowman probe + No Ruler	Bowman Probe + Ruler (Gold Standard)	Graduated Bowman Probe
1L (Lower)	4	5	7	6
1R (Upper)	0.5	1	2.5	2.5
2L(Lower)	2	1	2	2
2R(Upper)	1	2	4	3.5
3L(Lower)	2	1.5	2	2
3R(Upper)	4	2.5	3	3
4L(Lower)	10	8	8	7.5
4R(Upper)	13	18	15	12.5
5L(Lower)	12	6	5	7
5R(Upper)	15	12	11	10

Resident 2

Station #	Estimated (no measurements)	Bowman probe + No Ruler	Bowman Probe + Ruler (Gold Standard)	Graduated Bowman Probe
1L (Lower)		15	10	16
1R (Upper)		4	4	5
2L(Lower)		7	8	12.5
2R(Upper)		3	4	5
3L(Lower)		13	13	10
3R(Upper)		6	6	5
4L(Lower)		20	14	15
4R(Upper)		5	19	24
5L(Lower)		15	11	12
5R(Upper)		10	14	12.5

```
% Inputs
x = [6 2.5 2 3.5 2 3 7 10 5 2.5 1.25 3 2 3 0 11]; % graduated probe
y = [7 2.5 2 4 2 3 5 11 5 3 2 3 2 3 0 11]; % standard method
delta = 0.5; % equivalence margin (e.g., ±1 mm)
alpha = 0.05;
% Paired differences
d = x - y;
n = length(d);
% Stats
mean_d = mean(d);
sd_d = std(d);
se_d = sd_d / sqrt(n);
df = n - 1;
% 90% CI for TOST
t_crit = tinv(1 - alpha, df);
ci_low = mean_d - t_crit * se_d;
ci_high = mean_d + t_crit * se_d;
```

```
% TOST p-values
t1 = (mean_d + delta) / se_d;
p1 = 1 - tcdf(t1, df);
t2 = (mean_d - delta) / se_d;
p2 = tcdf(t2, df);
% Display results
fprintf('Mean difference: %.4f\n', mean_d);
fprintf('90%% CI: [%.4f, %.4f]\n', ci_low, ci_high);
fprintf('Equivalence bounds: [%.4f, %.4f]\n', -delta, delta);
fprintf('p1 = %.4f, p2 = %.4f\n', p1, p2);
if (p1 < alpha) && (p2 < alpha)
  disp('Equivalence established');
else
  disp('Equivalence NOT established');
end
figure;
hold on;
% Plot equivalence bounds
h1 = yline(delta, '--r', 'LineWidth', 1.5);
h2 = yline(-delta, '--b', 'LineWidth', 1.5);
% Plot mean difference
plot(1, mean_d, 'ko', 'MarkerFaceColor', 'k', 'MarkerSize', 8);
% Plot confidence interval as error bar
errorbar(1, mean_d, mean_d - ci_low, ci_high - mean_d, ...
  'k', 'LineWidth', 2, 'CapSize', 10);
% Formatting
xlim([0.5 1.5]);
xticks([]);
ylabel('Difference (Graduated - Standard)');
```

```
title('Paired TOST Equivalence Test');
legend([h1, h2], {'Upper Bound (+\Delta)', 'Lower Bound (-\Delta)'})
grid on;
hold off;
```

Appendix E: Tissue Pull Testing Raw Test Data and MATLAB Code

Table: Percent Disruption of each probe type and size for three trials (A, B, and C)

Probe Size	gA	gB	gC	uA	uB	uC
1	0.24	0.61	0.05	0.2	0.12	0.04
2	0.74	0.56	0.39	0.19	0.16	0.01
7	0.07	0.07	0.08	0.07	0.06	0.06
8	0.05	0.07	0.05	0.06	0.08	0.03
4	0.03	0.01	0.1	0.04	0.01	0.08

```
%% Equivalence margin (YOU must define this)
delta = 0.1; % change as needed
%% Sample sizes
nx = length(x);
ny = length(y);
%% Means
mx = mean(x);
my = mean(y);
diff_mean = mx - my;
%% Variances
vx = var(x);
vy = var(y);
%% Standard error (Welch)
se = sqrt(vx/nx + vy/ny);
%% Welch-Satterthwaite degrees of freedom
```

BME Design: 301

```
df = (vx/nx + vy/ny)^2 / ((vx^2/(nx^2*(nx-1))) + (vy^2/(ny^2*(ny-1))));


%% TOST t-statistics
t1 = (diff_mean + delta) / se; % lower bound test
t2 = (diff_mean - delta) / se; % upper bound test
%% One-sided p-values
p1 = 1 - tcdf(t1, df);
p2 = tcdf(t2, df);
%% Decision
alpha = 0.05;
if (p1 < alpha) && (p2 < alpha)
result = "EQUIVALENT (TOST passed)";
else
result = "NOT equivalent (TOST failed)";
end
%% 90% Confidence Interval (TOST equivalent check)
tcrit = tinv(1 - alpha, df);
CI_low = diff_mean - tcrit * se;
CI_high = diff_mean + tcrit * se;
%% Output
fprintf("Group 1 mean: %.4f\n", mx);
fprintf("Group 2 mean: %.4f\n", my);
fprintf("Difference (x - y): %.4f\n\n", diff_mean);
fprintf("SE: %.4f\n", se);
fprintf("df: %.2f\n\n", df);
fprintf("TOST p1 (lower): %.4f\n", p1);
fprintf("TOST p2 (upper): %.4f\n\n", p2);
fprintf("90%% CI: [%.4f, %.4f]\n", CI_low, CI_high);
fprintf("Equivalence margin: ±%.4f\n\n", delta);
```

fprintf("RESULT: %s\n", result);

Appendix F: Uniformity Testing Data

	First Mark Length	Avg. Mark Length	Std Mark Length	Avg Mark Width	Std Mark Width		Mark 1 L	Mark 2 L	Mark 3 L	Mark 4 L	Mark 1 W	Mark 2 W	Mark 3 W	Mark 4 W
Probe 0000	**2.921**	**2.6155**	**0.204581687**	**0.119**	**0.02**		**2.921**	**2.5**	**2.541**	**2.5**	**0.149**	**0.109**	**0.109**	**0.109**
Probe 000	**2.84**	**2.57925**	**0.175517093 2**	**0.15925**	**0.0205**		**2.84**	**2.459**	**2.516**	**2.502**	**0.149**	**0.149**	**0.19**	**0.149**
Probe 00	**2.99**	**2.63625**	**0.238001925 8**	**0.1665**	**0.038820097 89**		**2.99**	**2.473**	**2.541**	**2.541**	**0.19**	**0.19**	**0.109**	**0.177**
Probe 0	**2.733**	**2.5685**	**0.111356784**	**0.126**	**0.019782146 83**		**2.733**	**2.5**	**2.541**	**2.5**	**0.149**	**0.109**	**0.11**	**0.136**
Probe 1A	**2.948**	**2.6255**	**0.216045519 9**	**0.2035**	**0.036927857 6**		**2.948**	**2.502**	**2.504**	**2.548**	**0.149**	**0.217**	**0.217**	**0.231**
Probe 1B	**2.964**	**2.648**	**0.210673523 1**	**0.129**	**0.023094010 77**		**2.964**	**2.542**	**2.541**	**2.545**	**0.109**	**0.149**	**0.109**	**0.149**
Probe 2A	**2.69**	**2.56775**	**0.090001388 88**	**0.16625**	**0.020613506 9**		**2.69**	**2.5**	**2.581**	**2.5**	**0.19**	**0.149**	**0.177**	**0.149**
Probe 2B	**2.841**	**2.60775**	**0.156757509 1**	**0.156**	**0.014**		**2.841**	**2.545**	**2.502**	**2.543**	**0.149**	**0.177**	**0.149**	**0.149**

Probe 3A	**2.881**	**2.61625**	**0.177530044**	**0.13225**	**0.020056171 12**		**2.881**	**2.501**	**2.542**	**2.541**	**0.149**	**0.122**	**0.109**	**0.149**
Probe 3B	**2.732**	**2.56275**	**0.118009533 5**	**0.1695**	**0.023671361 04**		**2.732**	**2.46**	**2.543**	**2.516**	**0.149**	**0.149**	**0.19**	**0.19**
Probe 3C	**2.692**	**2.569**	**0.084194219 91**	**0.12225**	**0.018856917 39**		**2.692**	**2.501**	**2.542**	**2.541**	**0.122**	**0.109**	**0.149**	**0.109**
Probe 3D	**2.717**	**2.569**	**0.100119928 1**	**0.1695**	**0.023671361 04**		**2.717**	**2.513**	**2.503**	**2.543**	**0.19**	**0.19**	**0.149**	**0.149**
Probe 4A	**3.057**	**2.653**	**0.269870339 2**	**0.129**	**0.023094010 77**		**3.057**	**2.514**	**2.541**	**2.5**	**0.109**	**0.109**	**0.149**	**0.149**
Probe 4B	**2.541**	**2.51425**	**0.033079449 81**	**0.146**	**0.027976180 34**		**2.541**	**2.473**	**2.541**	**2.502**	**0.149**	**0.177**	**0.149**	**0.109**
Probe 4C	**2.364**	**2.496**	**0.088**	**0.139**	**0.02**		**2.364**	**2.54**	**2.54**	**2.54**	**0.109**	**0.149**	**0.149**	**0.149**
Probe 4D	**2.583**	**2.54225**	**0.033480093 59**	**0.14925**	**0.033069371 53**		**2.583**	**2.501**	**2.543**	**2.542**	**0.149**	**0.109**	**0.149**	**0.19**
Probe 5A	**2.758**	**2.578**	**0.121213310 6**	**0.15925**	**0.0205**		**2.758**	**2.5**	**2.541**	**2.513**	**0.19**	**0.149**	**0.149**	**0.149**
Probe 5B	**2.948**	**2.62225**	**0.218025036 8**	**0.1525**	**0.028053520 28**		**2.948**	**2.5**	**2.5**	**2.541**	**0.122**	**0.149**	**0.149**	**0.19**

Probe 6A	**2.759**	**2.579**	**0.1212133106**	**0.109**	**0**		**2.759**	**2.501**	**2.542**	**2.514**	**0.109**	**0.109**	**0.109**	**0.109**
Probe 6B	**2.907**	**2.612**	**0.1987947015**	**0.146**	**0.006**		**2.907**	**2.5**	**2.554**	**2.487**	**0.149**	**0.137**	**0.149**	**0.149**
Probe 7A	**2.65**	**2.56175**	**0.060096450 26**	**0.1695**	**0.023671361 04**		**2.65**	**2.541**	**2.515**	**2.541**	**0.149**	**0.149**	**0.19**	**0.19**
Probe 7B	**2.542**	**2.5245**	**0.020338797 08**	**0.1595**	**0.038820097 89**		**2.542**	**2.514**	**2.541**	**2.501**	**0.19**	**0.149**	**0.109**	**0.19**
Probe 7C	**2.649**	**2.558**	**0.063529520 7**	**0.16625**	**0.020613506 9**		**2.649**	**2.541**	**2.541**	**2.501**	**0.149**	**0.149**	**0.19**	**0.177**
Probe 7D	**2.541**	**2.53575**	**0.014591664 29**	**0.1595**	**0.038820097 89**		**2.541**	**2.514**	**2.543**	**2.545**	**0.109**	**0.149**	**0.19**	**0.19**
Probe 8A	**2.691**	**2.56175**	**0.092019472 58**	**0.16625**	**0.020613506 9**		**2.691**	**2.473**	**2.541**	**2.542**	**0.149**	**0.149**	**0.19**	**0.177**
Probe 8B	**2.88**	**2.612**	**0.182162930 7**	**0.14925**	**0.033069371 53**		**2.88**	**2.473**	**2.554**	**2.541**	**0.149**	**0.109**	**0.149**	**0.19**
Probe 8C	**2.921**	**2.636**	**0.192857460 3**	**0.1695**	**0.023671361 04**		**2.921**	**2.501**	**2.582**	**2.54**	**0.149**	**0.19**	**0.19**	**0.149**
Probe 8D	**3.099**	**2.6745**	**0.283287251 2**	**0.1865**	**0.028053520 28**		**3.099**	**2.515**	**2.541**	**2.543**	**0.19**	**0.19**	**0.149**	**0.217**

Avg	**2.779964286**	**2.586660714**	**0.138405319 5**	**0.1526875**	**0.023786404 89**		**Avg no First:**	**2.52222619**					
Std	**0.1770426779**	**0.4116095374**		**0.021353140 22**			**Std no First:**	**0.025628180 64**					
Length Avg Error:	**0.09269642857**					**Error:**	**0.421**	**0**	**0.041**	**0**			
Length Error:	**3.71%**						**0.34**	**0.041**	**0.016**	**0.002**			
							0.49	**0.027**	**0.041**	**0.041**			
Width Avg Error	**0.0234397321 4**						**0.233**	**0**	**0.041**	**0**			
Width Error:	**0.1535144144**	**15.35%**					**0.448**	**0.002**	**0.004**	**0.048**			
							0.464	**0.042**	**0.041**	**0.045**			
							0.19	**0**	**0.081**	**0**			
							0.341	**0.045**	**0.002**	**0.043**			
							0.381	**0.001**	**0.042**	**0.041**			
							0.232	**0.04**	**0.043**	**0.016**			

							0.192	**0.001**	**0.042**	**0.041**				
							0.217	**0.013**	**0.003**	**0.043**				
							0.557	**0.014**	**0.041**	**0**				
							0.041	**0.027**	**0.041**	**0.002**				
							0.136	**0.04**	**0.04**	**0.04**				
							0.083	**0.001**	**0.043**	**0.042**				
							0.258	**0**	**0.041**	**0.013**				
							0.448	**0**	**0**	**0.041**				
							0.259	**0.001**	**0.042**	**0.014**				
							0.407	**0**	**0.054**	**0.013**				
							0.15	**0.041**	**0.015**	**0.041**				
							0.042	**0.014**	**0.041**	**0.001**				
							0.149	**0.041**	**0.041**	**0.001**				
							0.041	**0.014**	**0.043**	**0.045**				
							0.191	**0.027**	**0.041**	**0.042**				
							0.38	**0.027**	**0.054**	**0.041**				
							0.421	**0.001**	**0.082**	**0.04**				

							0.599	**0.015**	**0.041**	**0.043**				

Appendix G: Autoclave Testing Raw Data

Bowman Probe size	not autoclaved (g)	autoclaved (g)	total weight lost (mg)
0000/000	1.7137	1.7125	1.2
00/0	1.7373	1.7351	2.2
1/2	1.8698	1.8695	0.3
3/4	1.9962	1.9955	0.7
5/6	2.0852	2.0867	-1.5
7/8	2.2513	2.2481	3.2

Appendix H: Laser Fixture Fabrication Protocol

Obtain the following

1. ½ inch end mill
2. steel chuck
3. 2 flute
4. ½ inch edgefinder
5. Level to fit the clamp so part is slightly above
6. rubber hammer

Fabrication

1. Place the aluminum piece under above the levels into the clamp
2. Fasten the clamp and hit with rubber hammer so the aluminum piece is secure and cannot move
3. attach the ½ inch endmill to the end of the chuck
4. set rpm to 1500
5. Make one pass on the edge short end of the aluminum piece to ensure that it is flat and repeat for the other side
6. remove the endmill from the chuck
7. place the edgefinder inside of the chuck
8. set rpm to 800
9. touch off the short end of the aluminum piece
10. zero x axis

11. raise the handle and move the edgefinder over 0.25 inches and zero again
12. repeat steps 9-11 for the long side of the aluminum except zeroing the y axis instead of the x
13. zero the z axis
14. remove the edgefinder
15. insert 2 flute into the chuck
16. set rpm to 1500
17. move the chuck down the y axis 1 inch towards the center of the piece
18. begin making a pass about 0.0025 inches deep using the z axis following the x axis
19. make a second pass following the same line but set the z axis to 0.0035 inches
20. move the chuck 0.73 inches over towards the center
21. repeat steps 18 and 19 except the z axis depth is 0.0015 inches and 0.0025 inches
22. repeat step 20
23. repeat steps 18 and 19 except the z axis depth is 0.001 inches and 0.0015 inches
24. use a deburring tool to remove any rough edges

Appendix I: Artificial Tear Solution Protocol

Obtain the following:

1. 1 Corning Pyrex 500 mL storage media bottle
2. 1 stir bar
3. 500 mL Deionized Water
4. 3.655 g NaCl
5. 0.745 g KCL
6. 0.0735 g $CaCl_2$ - $2H_2O$
7. 0.0510 g $MgCl_2$ - $6H_2O$
8. 0.08 g NH_4Cl
9. 1.97 g Albumin
10. 1 M HCl
11. 1 M NaOH
12. 1 Weigh boat
13. 6 Scoopula's
14. 1 Fischer Scientific Weigh Scale
15. 1 ThermoFisher IsoTemp magnetic stirrer and hot plate
16. 1 pH Meter

Preparation:

1. Add 500 mL deionized water to the Corning Pyrex 500 mL storage media bottle
2. Place the stir bar inside the bottle
3. Place the bottle on top of the ThermoFisher IsoTemp magnetic stirrer and hot plate
4. Set the magnetic stirrer to 200 rpm and temperature to 37℃
5. Measure the necessary amount of each chemical on the weigh scale

6. Add in the chemicals using 1 scoopula per powder
7. Repeat steps 5 & 6 for chemicals 4-8
8. When adding Albumin, add little amounts and wait for powder to completely dissolve (if entire quantity of Albumin is added at once, it will denature and not fully dissolve)
9. Measure the pH of the solution
10. Add in drops of 1 M NaOH if the pH is below 7.4, and drops of 1 M HCl if the pH is above 7.4
11. pH balance solution to 7.4

Appendix J: Agar+Gelatin+Charcoal Soft Tissue Mimic Protocol

Materials:

1. 600 mL beaker
2. 10000 mL graduated cylinder
3. 100 mL graduated cylinder
4. 3 Weigh boats
5. 1 20μm filter
6. 8g Agar
7. 24g gelatin
8. 1g of charcoal powder (or 1 charcoal stick)
9. 1 stir/hot plate
10. 15 25mL centrifuge flasks
11. 1 stir bar
12. 1 scapula
13. 1 20℃ fridge

Preparation:

1. Obtain 600 mL beaker
2. Fill the beaker with 200 mL of DI water using a 1000 mL graduated cylinder.
3. Place the Beaker on a stir plate and heat till water temperature reaches approx 90 deg C
4. While water is heating, weigh out 8g agar and 24g gelatin on weigh boats
5. Place a stir bar into the beaker and create a vortex in the center of the beaker, approx 600 rev/min.
6. Slowly incorporate agar into beaker and mix until dissolved
7. Once dissolved, bring the heat of the stir plate down to 50 deg C and let the beaker cool.
8. Obtain 50 mL of DI water in a 100 mL graduated cylinder.
9. Sprinkle gelatin into 50 mL to allow blooming.

10. Once the bloomed gelatin is translucent, and Agar solution has come down between 50 and 60 Deg C, slowly incorporate gelatin into solution vortex until fully dissolved.
11. If you have charcoal powder, skip to step 15. If you have a charcoal stick, continue to the next step.
12. Break off a small piece of the charcoal stick and place into mortar and pestle
13. Grind up charcoal at a medium vigor for a few minutes until relatively fine. (important to not make too fine as will not be distinguishable for the computer)
14. Obtain a 20 micron filter, a coffee filter for example, and sift charcoal powder through the filter.
15. Using powder, weight out 1.0 g of charcoal powder.
16. Lower stir rate to approx 300 rev/min and incorporate charcoal into the agar+gelatin mixture.
17. Once completely incorporated, the solution should look very dark.
18. Using a graduated cylinder, bring the volume of solution to 400 mL using DI.
19. Using a 400 mL solution, fill 15 25mL cell culture flasks.
20. Place flasks into the fridge overnight to allow solidification.